1979

An experimental study of dropwise condensation on vertical discs.

Perkins, Kevin Patrick

Monterey, California : Naval Postgraduate School

AN EXPERIMENTAL STUDY OF DROPWISE CONDENSATION ON VERTICAL DISCS

Kevin Patrick Perkins

NAVAL POSTGRADUATE SCHOOL
Monterey, California

THESIS

AN EXPERIMENTAL STUDY OF
DROPWISE CONDENSATION ON VERTICAL DISCS

by

Kevin Patrick Perkins

December 1979

Thesis Advisor: Paul J. Marto

Approved for public release; distribution unlimited

Unclassified

SECURITY CLASSIFICATION OF THIS PAGE (When Data Entered)

REPORT DOCUMENTATION PAGE		READ INSTRUCTIONS BEFORE COMPLETING FORM
1. REPORT NUMBER	2. GOVT ACCESSION NO.	3. RECIPIENT'S CATALOG NUMBER
4. TITLE (and Subtitle) An Experimental Study of Dropwise Condensation on Vertical Discs		5. TYPE OF REPORT & PERIOD COVERED Master's Thesis; December 1979 6. PERFORMING ORG. REPORT NUMBER
7. AUTHOR(s) Kevin Patrick Perkins		8. CONTRACT OR GRANT NUMBER(s)
9. PERFORMING ORGANIZATION NAME AND ADDRESS Naval Postgraduate School Monterey, California 93940		10. PROGRAM ELEMENT, PROJECT, TASK AREA & WORK UNIT NUMBERS
11. CONTROLLING OFFICE NAME AND ADDRESS Naval Postgraduate School Monterey, California 93940		12. REPORT DATE December 1979 13. NUMBER OF PAGES 91 pages
14. MONITORING AGENCY NAME & ADDRESS(if different from Controlling Office) Naval Postgraduate School Monterey, California 93940		15. SECURITY CLASS. (of this report) Unclassified 15a. DECLASSIFICATION/DOWNGRADING SCHEDULE
16. DISTRIBUTION STATEMENT (of this Report) Approved for public release; distribution unlimited		
17. DISTRIBUTION STATEMENT (of the abstract entered in Block 20, if different from Report)		
18. SUPPLEMENTARY NOTES		
19. KEY WORDS (Continue on reverse side if necessary and identify by block number) Dropwise condensation, organic promoters, thickness dependence.		

20. ABSTRACT (Continue on reverse side if necessary and identify by block number)

Three hydrophobic coating systems were tested for their ability to promote permanent dropwise condensation of steam at 21 KPa (3 psia). The coatings used were: (1) Nedox, a Teflon coating that uses a porous nickel substrate to improve adhesion, (2) Sputtered Teflon, and (3) C-6 fluoroepoxy, a protective coating developed for naval aircraft. Copper-nickel discs, 32 mm in diameter, were tested with all three coatings. In

DD FORM 1 JAN 73 1473 (Page 1) EDITION OF 1 NOV 65 IS OBSOLETE S/N 0102-014-6601

Unclassified

SECURITY CLASSIFICATION OF THIS PAGE (When Data Entered)

20. (Cont'd)

addition, copper and titanium discs were tested with the sputtered Teflon coating. Coating thickness was varied from 0.08 to 25.0 microns.

The coatings tested provided only moderate improvements in heat transfer. The 0.08 micron coating of sputtered Teflon on copper-nickel provided only a 58 percent improvement in the heat transfer coefficient over filmwise. A chemically promoted specimen tested in the same experimental apparatus gave a 500 percent improvement in the heat transfer coefficient.

All coatings tested showed surface deterioration after two to ten hours of testing, and none would be considered a practical permanent promoter of dropwise condensation.

Approved for public release; distribution unlimited

AN EXPERIMENTAL STUDY OF DROPWISE CONDENSATION ON VERTICAL DISCS

by

Kevin Patrick Perkins
Lieutenant, United States Navy
B.S., University of Illinois, 1970

Submitted in partial fulfillment of the
requirements for the degree of

MASTER OF SCIENCE IN MECHANICAL ENGINEERING

from the

NAVAL POSTGRADUATE SCHOOL
December 1979

ABSTRACT

Three hydrophobic coating systems were tested for their ability to promote permanent dropwise condenstion of steam at 21 KPa (3 psia). The coatings used were: (1) Nedox, a Teflon coating that uses a porous nickel substrate to improve adhesion, (2) Sputtered Teflon, and (3) C-6 fluoroepoxy, a protective coating developed for naval aircraft. Copper-nickel discs, 32 mm in diameter, were tested with all three coatings. In addition, copper and titanium discs were tested with the sputtered Teflon coating. Coating thickness was varied from 0.08 to 25.0 microns.

The coatings tested provided only moderate improvements in heat transfer. The 0.08 micron coating of sputtered Teflon on copper-nickel provided only a 58 percent improvement in the heat transfer coefficient over filmwise. A chemically promoted specimen tested in the same experimental apparatus gave a 500 percent improvement in the heat transfer coefficient.

All coatings tested showed surface deterioration after two to ten hours of testing, and none would be considered a practical permanent promoter of dropwise condensation.

TABLE OF CONTENTS

LIST OF TABLES

LIST OF FIGURES

NOMENCLATURE

A - Area (m^2)

A_s - Surface area (m^2)

h_e - Expected heat transfer coefficient (w/m^2C)

h_{fg} - Enthalpy (J/kg)

k - Thermal conductivity (w/m C)

$\dot{m}$ - Mass flow rate (kg/s)

p - Pressure (KPa)

Q - Heat flux (w/m^2)

T - Temperature (C)

T_s - Surface temperature of specimen (^oC)

T_v - Vapor temperature (^oC)

ΔT - $T_v - T_s$ (C)

ρ - Fluid density (kg/m^3)

ACKNOWLEDGMENT

The work presented here has been supported by Mr. Charles Miller, Naval Sea Systems Command (Code 05R).

A special note of appreciation is extended to Ken Mothersell, Tom Christian, Tom Kellogg and Ron Longueira for their technical assistance.

I am especially grateful to Professor Paul J. Marto, my thesis advisor, for his invaluable guidance.

I. INTRODUCTION

A. BACKGROUND INFORMATION

During the past twenty years the cost of construction of a rankine cycle power plant, marine or stationary, has risen dramatically. These increases in cost have lead to a realization of the need for more efficient and smaller boilers and condensers. The need is even greater in the marine application because design is constrained by both cost and size. The main propulsion plant and auxiliary equipment of modern warships consume twenty to forty percent of the total ship volume. Any reduction in propulsion plant size will provide a twofold benefit. One, there will be a reduction in the initial cost. Two, more space will be available for other purposes. The second is an important long term benefit. It can mean greater operating range, more weapons capability or perhaps a smaller ship. In short, it means greater design flexibility.

There has been some reduction in the size of marine propulsion plants, but most of the effort has been in the area of boiler design. Boiler operating pressures and temperatures have been increased, thus reducing size. There have also been modifications in air flow through the boiler that have improved efficiency. The marine condenser has remained basically unchanged for the past thirty years.

Search [1] did a feasibility study to determine what improvements could be made in the marine condenser. His results

indicate that more than thirty percent improvement in heat transfer could be expected if the condensation was dropwise vs. filmwise. This was based on a tenfold increase in the outside heat transfer coefficient, not unreasonable for dropwise condensation. A corresponding reduction of thirty percent in condenser weight and a twenty-three percent reduction in condenser volume could be expected. Unfortunately dropwise condensation is not as stable or well understood as filmwise condensation.

B. FILMWISE CONDENSATION

Filmwise condensation is the normal mode of condensation on all condenser materials. A sheet of water forms on the condenser surface because of the high surface energy of the condenser materials. Further condensation takes place on the sheet of water, which introduces an additional resistance to heat transfer. This is a relatively high resistance, so filmwise condensation is not strongly affected by lower order resistances such as fouling of the condenser surface or the presence of non-condensable gases. It is a stable and predictable mode of heat transfer.

C. DROPWISE CONDENSATION

Dropwise condensation occurs when, by artificial means (promoters) the surface energy of the condenser material is lowered. This causes the water to form on the surface in droplets; hence the name. The droplets form rapidly, and fall off, resulting in a dramatic reduction in the resistance

to heat transfer. Because of this, dropwise condensation is very sensitive to other resistances, such as non-condensable gases and surface fouling.

Two theories have been proposed to explain the dropwise phenomenon. Jakob [2] believed that a very thin liquid film formed on the surface, then coalesced, forming drops that then rolled off. The second theory, developed by Tammam and Boehme [3] is the nucleation theory. It says that the drops are formed at nucleation sites on the surface and that the area between the drops is dry. The nucleation theory is generally accepted today.

Compared with filmwise condensation, dropwise is far more difficult to study. The process of drop formation and removal from the surface is an unsteady and non-uniform phenomenon. Graham and Aerni [4] described what can be called the life of a drop. A drop starts at a nucleation site and grows rapidly by condensation. As the drop grows, it comes in contact with many other small drops. The drops coalesce, forming larger drops. When a drop is about 0.1 mm in diameter, direct condensation almost stops except in the vicinity of the interface of the liquid, vapor and condenser surface, where high heat transfer rates continue. The drop continues to grow, primarily by coalescence, until it reaches a critical size when surface tension is overcome by external forces, such as gravity or vapor shear, and the drop departs from the surface.

D. FACTORS THAT INFLUENCE DROPWISE CONDENSATION

Tanasawa [5] noted twenty-three factors that influence the heat transfer coefficient of dropwise condensation. Among

the most important are: (1) condenser surface roughness, (2) surface coating or promoter, (3) external forces, (4) thermal properties of the condenser material, and (5) non-condensable gases.

The first three factors work together to determine drop departure size. Drop departure diameter has been shown both by theory and experiment [5] to be related to the heat transfer coefficient. Smaller drop departure diameters yield higher heat transfer coefficients. The ideal condenser would have a mirror smooth surface with many small nucleation sites. The promoter would, ideally, be as thin as possible, a monomolecular layer thick, and would impart to the condenser surface a very low surface energy. Also, the external forces of gravity and vapor shear would act together to remove the droplets as rapidly as possible.

The effect of the fourth factor, condenser material thermal properties, is a highly debated subject. Hanneman and Mikic [6] have proposed a theory that there is an additional resistance to condensation because of the non-uniformity of dropwise condensation. They postulate that, because of the size and spacing of the drops on the surface, there is a non-uniformity in surface temperature and heat flux. The large drops, for example, act as insulators against the heat flux, while the small drops have a great heat flux through them. Figure 1 illustrates the effect on heat flux near the surface. The net result of this non-uniformity in heat flux is an additional resistance to heat transfer known as the constriction resistance. Low thermal conductivity

materials show greater non-uniformity in surface temperature because they allow less lateral heat transfer near the surface. As a result they have a higher constriction resistance. Hanneman and Mikic support this theory with data of their own and others. Rose [7] represents the opposite view. He believes the non-uniformities in surface heat flux are rapidly homogenized by the frequent coalescences between drops and that the effect of a constriction resistance, if present at all, is small. Rose supports his contention with data from several experiments. The question remains unresolved.

The fifth factor is the effect of non-condensables. It has long been known that non-condensables reduce the heat transfer coefficient of filmwise condensation. The effect of non-condensables on the heat transfer coefficient of dropwise condensation is even greater. Graham [8] showed a reduction of the heat transfer coefficient of over 1200 percent because of the presence of non-condensable gases.

The two factors that prevent practical application of dropwise condensation are the adverse effect of non-condensables and the lack of a permanent promoter. The first could be overcome by employing condenser designs that result in high vapor velocities, or vapor velocities large enough to remove or sweep away the gases. The second has yet to be adequately resolved.

E. PROMOTION OF DROPWISE CONDENSATION

The promotion of dropwise condensation can be accomplished in three ways: (1) by chemically promoting (i.e., wiping) the surface with a liquid chemical, (2) by injecting hydrophobic chemicals into the vapor, and (3) by permanently coating the

surface with a hydrophobic material. The first method is a laboratory technique, of little use in naval condensers. Though it provides excellent dropwise condensation, the promoter washes off in a matter of hours. The second technique is not acceptable because it introduces impurities into the boiler feedwater system that could plate out on the boiler tubes. Thus, the third technique of using permanent promoters becomes the center of interest for naval steam condensers. Presently there are two types of permanent coatings that show promise as dropwise promoters, noble metals and organic polymers.

1. Noble Metals

The noble metals offer a great advantage in longevity; however, there is some question about their non-wetting characteristics. Erb and Thelen [9] have found that gold will produce good dropwise condensation for more than a year. Wilkins, Bromley and Read [10], however, reported only filmwise condensation with a gold plated condenser tube. They attributed the dropwise condensation to the presence of impurities in the gold coating. This debate remains unresolved. Recently Woodruff and Westwater [11] using precisely controlled procedures, plated a copper disc with various thicknesses of gold. They found that a thickness of 0.02 microns produced filmwise condensation. As the thickness was increased, the mode of condensation gradually changed to dropwise. They found that a 2.0 micron coating produced perfect dropwise condensation. Even if gold is found to be a good permanent promoter, the cost and availability may not make it practical.

Woodruff and Westwater estimated a coating cost of 50 dollars per square meter. This is just the cost of the gold, and it is based on gold at 200 dollars per troy ounce.

2. Organic Polymers

The second method of producing permanent dropwise condensation is to use organic polymers. Tanasawa [5] considers this the most promising approach, especially in light of the developing coating technologies. Teflon has been used to promote dropwise condensation since the 1950's. The early efforts met with limited success. The techniques used to apply Teflon required thick coatings, and adhesion was often a problem. Smith [12] obtained only a 10 percent improvement in the overall heat transfer coefficient using Teflon promoted copper-nickel tubes. He also reported rapid degradation of the coating performance. Coxe [13], using a 12.5 micron thick coating, obtained slightly better results. He had a 22 percent improvement in the overall heat transfer coefficient, and reported no degradation of promoter performance in a 100 hour test. Recently, Manvel [14] used two new coating techniques to apply teflon to horizontal condenser tubes. Using a commercial coating, Nedox, which combines a very thin coating of teflon on a nickel base, Manvel obtained slightly better results than Coxe or Smith. He obtained a 27 percent improvement in the overall heat transfer coefficient and a 53 percent improvement in the steam side heat transfer coefficient. These are not, however, the dramatic improvements that would be expected from dropwise condensation.

Graham [8] found that while a copper disc with a 1.5 micron thick coating of Teflon gave excellent dropwise condensation, the heat transfer coefficient was only one third that of an identical chemically promoted surface. This drastic reduction can be attributed to the extra resistance to heat transfer introduced by the low thermal conductivity of the Teflon coating. He indicated that the solution was to reduce the thickness of the coating.

The development of new coating technologies has made Teflon more attractive. Vacuum deposition techniques can now be used to apply extremely thin coatings of Teflon.

F. PURPOSE OF STUDY

The purpose of this study was to examine the ability of three coatings to promote permanent dropwise condensation on 90-10 copper-nickel discs. The coatings tested were: (1) Nedox, a coating system developed by the General Magnaplate Corporation, (2) Teflon, applied by a sputtering technique that permitted very thin coatings, and (3) C-6 fluoroepoxy, developed by Dr. James Griffith of the Naval Research Laboratory. Coating thickness was varied in an effort to determine an optimum thickness for permanence and heat transfer. Additionally, the sputtered Teflon was applied to copper and titanium specimens to determine the effect of condenser material on the heat transfer coefficient. Finally, two specimens were polished to a mirror smooth surface to measure the effect of surface roughness. One was coated with Nedox, and the other was coated with C-6 fluoroepoxy.

II. EXPERIMENTAL APPARATUS

A. INTRODUCTION

The experiment apparatus was designed and built by Sharp [15]. It consisted of three major components: (1) the condensing chamber, (2) the support systems, and (3) the instrumentation. Figure 2 shows a schematic of the entire system.

B. CONDENSING CHAMBER

The condensing chamber was constructed using a thick walled Pyrex glass cross 457.2 mm by 304.8 mm. The chamber was designed so that boiling and condensation took place in the same closed chamber. At the bottom of the chamber, five 250 watt immersion heaters were used to boil the water. The power input to the heaters was controlled by a Powerstat variable transformer. An auxiliary condenser was installed in the upper portion of the chamber. This provided for control of the steam pressure and steam flow rate past the specimen.

The condenser test section was mounted on one side of the cross, and a heated viewport was mounted on the other side. This arrangement provided an excellent view of the specimen during the test runs. Mounted inside the chamber was a small (12.5cc) Teflon cup that was used to collect and measure the condensate from the specimen. Teflon was used because of its machinability and relative freedom from outgassing when hot. The connections for the vacuum system, manometer, thermocouples and auxiliary condenser were all made through

the top plate. Figure 3 illustrates the details of the condensing chamber.

1. Condenser Test Section

The condenser test section consisted of two main parts; the specimen, with its nylon retainer ring, and the specimen holder. The test specimens were designed so that both heat flux and surface temperature could be obtained from a knowledge of the temperature distribution within the piece. The specimen holder and retainer ring were designed to ensure one dimensional heat flow.

The test specimens were solid cylinders 15.24 mm long and 31.75 mm in diameter. Five thermocouple holes were drilled radially to a depth of 13.34 mm into each specimen. The holes were equally spaced, 2.54 mm apart, along the length of the specimen. In an effort to minimize the effect of thermal distortion induced by the thermocouple holes, the holes were not lined up but were rotated 72 degrees from each other. In addition to the five main thermocouples, two thermocouples were located 2.54 mm from the front surface, one at a radial depth of 5.08 mm and the other at 15.24 mm. These thermocouples were used to determine if there was any heat flux in the radial direction. All thermocouple holes were 0.57 mm in diameter. Because accurate placement of the thermocouple holes was essential to an accurate determination of surface temperature, two specimens were cut in half and the placement of four thermocouple holes was checked by using an optical microscope with a calibrated grid. The maximum deviation from the specified location was 0.005 mm (.002 in.). To

obtain this accuracy, a starter hole, 0.81 mm in diameter and 5.08 mm deep, was used in six of the seven thermocouple holes. Figure 4 shows details of the specimen and the thermocouple holes.

Originally, the specimens were pressed into a nylon retainer ring and then pinned in place with a 1.60 mm diameter drill bit. Nylon was chosen because of its low thermal conductivity and relative freedom from outgassing when hot. It was felt that the pressed fit would provide an adequate seal between the specimen and retainer ring. However, because of nylon's high thermal expansion coefficient, the ring expanded when heated to the operating temperature of 60^{o}C, and an adequate seal was not provided. This allowed cooling water to run past the specimen and into the condensing chamber. The problem was solved by inserting a 0.127 mm thick piece of stainless steel shim stock between the nylon retained ring and the specimen holder. This provided a positive vacuum seal, yet did not significantly affect heat transfer. Figure 5 shows the details of the nylon ring.

2. Specimen Holder

The specimen holder was designed to place the specimen in the path of the steam flow, and to provide impingement cooling to the specimen. The specimen holder was constructed of nylon. It was made in two pieces, the front and rear chambers. The front chamber held the specimen and provided the water passage for cooling the specimen. The rear chamber provided the inlet and outlet cooling water passage. Figure 6 shows details of the specimen holder.

C. SUPPORT SYSTEMS

Three support systems were required for the operation of the condensing chamber: (1) the cooling water system, (2) the refrigeration/heating system, and (3) the vacuum system.

The cooling water system was used to remove heat from the test specimen and the auxiliary condenser. It consisted of a 1/3 horsepower pump, a large reservoir (863.6 mm by 330.2 mm by 304.8 mm), and a flowmeter. Mounted inside the reservoir were a refrigeration coil, and two 250 watt immersion heaters. This arrangement provided for very precise control of cooling water temperature, and flow to the specimen.

The vacuum system was used to maintain the desired pressure in the condensing chamber. It also served to vent non-condensables from the chamber. The vacuum system consisted of a Duo-seal mechanical vacuum pump, a moisture separator and a bleed valve that could be used to control the vacuum pressure in the chamber.

D. INSTRUMENTATION

1. Temperature

The following temperatures were monitored: (1) the temperature profile in the specimen, (2) the liquid and vapor temperatures in the condensing chamber, and (3) the cooling water inlet and outlet temperatures.

In all cases, stainless steel sheathed, copper-constantan thermocouples were used. The seven thermocouples used to measure the temperature profile in the specimen were all 0.508 mm diameter sheathed, with ungrounded junctions.

The small size and ungrounded junction acted to minimize the uncertainty of the hot junction location in the specimen.

All thermocouples were connected to a Hewlett Packard 2010C Data Acquisition System that was used to record all temperature data. This system was calibrated using a Rosemount Engineering Company Model 913A variable temperature bath. Water was the working medium. The temperature in the bath was measured using a Platinum Resistance Thermometer connected to a high precision Rosemount commutating bridge model 920A. This system provided an accuracy of $\pm$ 0.002^{o}C, and was used as the standard for calibration.

A computer program utilizing the IBM Scientific Subroutine INTRPL was used to convert millivolt readings from the thermocouples to degrees centigrade. The subroutine utilized a piecewise cubic interpolation scheme through the calibration points to provide a smooth calibration curve. The calibration curve accuracy was considered to be $\pm$ 0.05^{o}C.

2. Flow Rate

The flow rate of the cooling water was monitored by a Fischer and Porter Precision Bore Flowrater, with a maximum flow rate of 0.70 kg/s.

3. Pressure

Chamber pressure was monitored by using a standard U-tube mercury manometer calibrated in millimeters.

E. PERMANENT COATINGS

Three types of permanent coatings were used in this study. Copper-nickel specimens were used with all three. The coatings

were: (1) C-6 fluoroepoxy, (2) Nedox, and (3) sputtered Teflon. The sputtered Teflon was also applied to copper and titanium specimens. Table I lists nomenclature, nominal or requested coating thickness, and measured coating thickness for all specimens used in this study. For the specimens coated with the C-6 fluoroepoxy, there was a significant difference between the nominal coating thickness and the measured coating thickness. This difference was attributed to the method used to coat the specimens.

1. C-6 Fluoroepoxy

C-6 fluoroepoxy was developed as a protective coating for naval aircraft by Dr. James Griffith of the Naval Research Laboratory's Chemistry Division. It is hydrophobic, soil resistant and inert. Four specimens were coated with C-6 fluoroepoxy. The specimens were coated by dipping them in a standard solution of C-6 fluoroepoxy with an equivalent amount of Si-2 silicone amine as the curing agent. The solvent was Freon TF. The thickness of the coating was increased by repeated dippings of the specimen in the solution.

Before coating, one of the specimens was polished to a mirror smooth finish. The remaining three were left with a machined surface. Three different coating thicknesses were requested. Table I shows the nominal thickness values and the values obtained by cutting the specimens in half with a waffering saw, and examining the edges with a Scanning Electron Microscope (SEM). All the specimens examined showed great non-uniformity of coating thickness; for that reason

there is a great uncertainty in the coating thickness, approximately ± 5.0 microns.

2. Nedox

Nedox is a commercially available coating technique developed by the General Magnaplate Corporation of Linden, New Jersey (GMP). Nedox is a proprietary process of GMP in which a hard surface nickel alloy is deposited on a copper-nickel surface. The structure of the deposit is porous, and a series of proprietary processes enlarge the microstructure to accept controlled infusion of Teflon. Four specimens received the Nedox coating. (Specimen G2, with a nominal coating thickness of 3.0 microns, was not coated with the rest of the specimens, and was received too late to be adequately evaluated. It is, therefore, not included in the data.) Table I shows the nominal and measured coating thicknesses.

Examination of the GMP coatings under the SEM prior to testing revealed that the Nedox coating was discontinuous on Specimen G1. This specimen had the thinnest (3.0 micron thick) coating and a polished surface below that coating. The other two specimens, G3 and G4, with nominal 5.0 and 10.0 micron thick coatings, respectively, had continuous coatings. The coatings were difficult to examine on the SEM because Teflon is an electrical insulator. This caused a static charge to build up rapidly on the specimen during scanning which blurred the image. Specimen G4 tended to blur more rapidly, indicating the thickness of the Teflon coating was greater than G3. After testing, the specimens were cut in half with a waffering saw and examined under the SEM to

determine coating thickness. The average coating thickness of the nickel appeared to be very close to the nominal value, though there was significant local variance. It was very difficult to determine the nickel-Teflon interface, and evaluate the Teflon thickness. Therefore, there is a large uncertainty in the thickness of the Teflon coating, approximately $\pm$ 0.2 microns.

3. Sputtered Teflon

Teflon was applied by a vacuum deposition sputtering process at Hohman Plating and Manufacturing Company of Dayton, Ohio. This resulted in an ultra-thin coating. A total of six specimens were coated in this manner, two each of copper, titanium, and copper-nickel. All surfaces were left as machined. Two coating thicknesses were used, 0.08 and 0.13 microns. By its very nature, the sputtering technique provides precise control of thickness, so the nominal values for thickness were taken to be accurate. The specimens were examined using an optical microscope prior to testing, because the SEM was inoperative when these specimens were received. The coatings were not continuous. The Teflon appears to have formed at nucleation sites and then grown outward from them. The coverage was estimated to be 80 percent complete for the 0.08 micron thickness, and 85 percent complete for the 0.13 micron thickness.

F. CHEMICALLY PROMOTED SPECIMENS

Two chemically promoted specimens were used in this experiment. They were polished so that they had approximately the

same surface smoothness as the specimens with permanent coatings. The promoter used was n-octadecyl mercaptan in octanoic acid. It was applied to the surface with a cotton swab and the surface was rinsed with distilled water. The specimen was tested immediately after promoter application.

G. UNCOATED SPECIMEN

To provide a reference or standard to be used to measure the heat transfer enhancement, one specimen was not coated, but left as machined. This specimen was washed with an industrial detergent and a solution that consisted of equal parts of sodium hydroxide and ethyl alcohol. The specimen was then completely rinsed with distilled water. This procedure ensured filmwise condensation on the surface.

III. EXPERIMENTAL PROCEDURES

A. OPERATING PROCEDURES

The following procedures were used to startup and operation of the experimental apparatus.

1. Approximately 24 hours prior to an experimental run, the data acquisition system and electronic ice point were turned on.

2. The condensing chamber was filled with distilled water to a level of five centimeters above the immersion heaters.

3. The specimen was mounted in the specimen holder; the thermocouples were inserted and secured in place with a nylon strap, and the specimen holder was mounted in the chamber. Vacuum was drawn down to 100 mm mercury, the isolation valves closed and the vacuum pump secured. The mercury manometer was checked after a 30 minute period. Vacuum was considered satisfactory if a one millimeter or less drop in pressure was observed.

4. The low pressure air supply and heating element to the observation port were turned on.

5. The cooling water and refrigeration systems were activated. The refrigeration system was left on until the water in the reservoir was approximately seven degrees centigrade. The cooling water to the specimen was turned on full flow.

6. The immersion heaters in the chamber were turned on and the power set to 70 percent, 900 watts.

7. When the water temperature reached sixty degrees centigrade, the vacuum system was activated. On the first set of trial runs, vacuum pressure in the chamber was controlled using the bleed valve located between the moisture separator and the vacuum pump. It is believed that this procedure allowed air to be sucked back through the moisture separator into the condenser chamber. After some experimentation, it was found that the best way to control vacuum and eliminate non-condensables was to secure the auxiliary condenser and bleed valve. Pressure was then controlled solely with the Powerstat regulator to the immersion heaters. It was found that during steady state operation a Powerstat setting of 60 percent plus or minus 4 percent would maintain pressure and temperature within the limits required.

8. Once an equilibrium state had been reached, thermocouple voltages were checked and recorded. If it was the first run for a coating or specimen material, the rate of condensate produced was measured. This was done by measuring the time required to fill the 12.5 cc Teflon cup. It was done to verify the values of thermal conductivity used for the calculation of heat flux by Fourier's Law. It was originally intended to measure the condensate flow rate for each specimen tested. The system worked fine during trial runs when the bypass valve was used to control pressure. The powerstat setting required to maintain temperature resulted in a low

boiling rate. With the bypass closed, as it was for all experimental runs, the high power setting and boiling rate would cause water from the boiling section of the chamber to occasionally splash into the Teflon cup, thus confounding the measurement. As a result, it took constant observation of the specimen and condensation cup to get a good measurement of condensate flow rate. Anytime water splashed into the cup, the run would be stopped and restarted. This increased the time to get a single data point to an unreasonable period. For this reason it was decided to measure the condensate flow rate on selected specimens only.

The heat flux was varied by increasing the cooling water temperature so the temperature difference ($T_v - T_s$) increased by approximately $0.5^{\circ}C$ for each data point. The ($T_v - T_s$) value was approximated by monitoring the voltages at the first and second thermocouple positions and calculating a rough slope to obtain the approximate T_s. At the lower heat flux ranges, the cooling water flow rate was also used to vary heat flux.

B. HEAT TRANSFER DATA REDUCTION

Both heat flux and surface temperature were determined using the temperature gradient in the specimen. The heat flux was determined using the one dimensional Fourier equation

$$\frac{Q}{A} = -k \frac{\Delta T}{\Delta X}$$

The surface temperature was obtained by extrapolating the temperature distribution inside the specimen to the

surface. The temperature gradients were linear and the method of least squares was used to provide the best fit line through the thermocouple data. Figure 7 shows the results of a typical run. As a check, the heat flux was also obtained by collecting and measuring the rate of condensate flow for selected specimens. The values obtained for heat flux agreed within 22 percent. Using the values for heat flux, surface temperature and vapor temperature, the heat transfer coefficient was obtained using Newton's Law of Cooling.

$$h = \frac{\frac{Q}{A}}{T_v - T_s}$$

IV. RESULTS AND DISCUSSION

A. INTRODUCTION

1. Treatment of Data

The technique of measuring the temperature gradient in a block and extrapolating the results to the surface was chosen because it was thought to provide the most accurate measure of the average surface temperature available. Even so, the uncertainties associated with the data were significant. The uncertainty for a typical data point was $\pm$ 0.25^{o}C for the thermal potential ($T_v - T_s$), and $\pm$ 2.2 kw/m^2 in heat flux. This gives an uncertainty in the heat transfer coefficient of $\pm$ 4.0 kw/m^{2o}C, or about 13 percent. Appendix A shows the methods used to calculate the uncertainties, and the range of values obtained. The results show the effect of these large uncertainties. The data points were scattered and several different curves could be fit to each set of data points. Past studies [8] have shown that for ($T_v - T_s$) greater than 0.3^{o}C, heat flux vs. ($T_v - T_s$) data for dropwise condensation can be treated as linear. For this reason, and to treat the data in an unbiased manner, a least squares straight line was fit through each set of data points.

The chemically promoted specimens transferred heat so well that the ability of the cooling water system to remove it became the limiting resistance in the system. In this situation the values of ($T_v - T_s$) obtained varied from 0.52

to 0.63°C for the copper-nickel specimen, which corresponded to a heat flux of about 80 kw/m^2. Therefore, the heat transfer coefficients for the five data points were averaged to obtain a value of 138 kw/m^2°C. This value was used for comparison with other data. All comparisons between data for permanent coatings were made based on a $(T_v - T_s)$ of 2°C, which corresponded to a heat flux of about 80 kw/m^2. The comparisons between data for the uncoated specimen and all other specimens were also made based on a $(T_v - T_s)$ of 2°C. This corresponded to a heat flux of 45 kw/m^2 for the uncoated specimen. If the comparison had been made at a heat flux of 80 kw/m^2, the resulting values for h/h_{un} (h/h_{un} is the ratio of the heat transfer coefficients for the test specimen vs. the uncoated specimen) would have been 20 percent higher.

2. Overview of Results

Table II shows the specimens tested with their physical characteristics and selected heat transfer data. The results show good agreement with existing data. The heat transfer coefficient for the chemically promoted copper-nickel specimen was 138 kw/m^2°C. The heat transfer coefficient for a similarly promoted copper specimen was 143 kw/m^2°C. These values are typical of dropwise condensation at this reduced pressure [8], and are six times the value obtained for the uncoated specimen. The uncoated specimen exhibited filmwise condensation and the heat transfer coefficient showed good agreement with one calculated using a Nusselt Analysis: 22.5 kw/m^2°C, for the uncoated specimen vs. 20.8 kw/m^2°C from the Nusselt Analysis.

Details of the Nusselt Analysis are shown in Appendix C. Figure 8 shows the plot of Q vs. $(T_v - T_s)$ data for the uncoated specimen.

As mentioned previously, Manvel [14] used the same permanent coatings that were tested in this experiment on horizontal tubes at the same pressure and temperature. A direct comparison of data is not possible because of differences in geometry. However, for comparable thicknesses, there was good agreement in the percentage improvement of the heat transfer coefficient for coated vs. uncoated specimens. For example, for a specimen with a 0.08 micron thick sputtered Teflon coating, Manvel obtained a 45 percent improvement over an uncoated tube. This study, for the same coating thickness, showed a 58 percent improvement.

B. PERFORMANCE OF PERMANENT COATINGS

1. C-6 Fluoroepoxy

The quality of dropwise condensation produced by C-6 fluoroepoxy was fair to poor.[1] All of the specimens tested showed degradation of performance in promoting dropwise condensation after two to three hours. The thicker coatings showed physical failure of the surface by cracking. It is believed that this was caused by the difference in thermal expansion between the copper-nickel disc and the coating.

---

[1]This qualitative comparison is based upon the visual behavior of the dropwise process, including the nucleation of microdrops, their coalescence, and large drop departure conditions.

Figure 9 shows the plots of Q vs. $(T_v - T_s)$ for the four specimens. Because of the large uncertainty in the data, and to treat all data from the permanent coatings in a consistent manner, it was decided to fit straight lines to the data points for each specimen. In some cases (i.e., N4) this does not provide the best fit curve for the data. The difference between the linear fit and the best fit is in all cases less than the uncertainty in the data.

2. Nedox

The Nedox coated specimens gave the best quality dropwise condensation. The specimens with the continuous coatings (G3 and G4) gave dropwise condensation as good as the chemically promoted specimens. The specimen with the thinnest and discontinuous coating showed good quality dropwise. Overall, they displayed only moderate increases in the heat transfer coefficient over the filmwise specimen. The Nedox specimens showed no reduction in their ability to promote dropwise condensation during runs of up to ten hours in length. They did, however, show some physical deterioration of the surface. Small pieces of Teflon coating were washed off all the specimens. This left the coating with a discontinuous appearance. Some Teflon appeared to have remained stuck in the porous surface of the nickel. There was no evidence of failure of the nickel subcoating. This could explain why the specimens showed no deterioration on dropwise performance, in spite of partial failure of the Teflon coating. Figure 10 shows the plots of Q vs. $(T_v - T_s)$ for the Nedox coatings.

3. Sputtered Teflon

Initially, the sputtered Teflon surfaces gave very good dropwise condensation, but not quite as good as the Nedox coated specimens. The quality of dropwise condensation began to deteriorate within two hours of operation. Several small patches of filmwise condensation appeared. The drop growth and coalesence was also slightly slower than the Nedox coated specimens. The heat transfer coefficients for the sputtered Teflon coatings were the highest recorded for the permanent promoters, but were still low for dropwise condensation. After four hours of operation, the surfaces showed signs of physical deterioration. The surface had dulled and small patches of Teflon had peeled away. Figure 11 shows the plots of Q vs. $(T_v - T_s)$ for the two sputtered Teflon coatings on Cu-Ni.

C. EFFECT OF COATING THICKNESS

1. Overview

The great advantage of chemical promoters, like n-octadecyl mercaptan in octanoic acid, is that they are only a monomolecular layer thick. Therefore, they do not induce a significant additional resistance to heat flux due to conduction through their thickness. The permanent promoters used in this experiment, Teflon and C-6 fluoroepoxy both have low thermal conductivities. Even though the coatings were thin by normal measure, ranging from 0.08 to 25.0 microns, the conduction resistance was significant, because of their low thermal conductivities.

One way to predict the increased resistance through the specimen was to assume the heat transfer coefficient for the chemically promoted copper-nickel specimen represented a value which could be used for a condensation resistance. This condensation resistance could then be added in series with the

conduction resistance of the permanent promoter to give an expected heat transfer coefficient. Appendix B shows the details of this calculation for a Teflon coated specimen. Figure 12 shows the results of this calculation graphically, with the expected heat transfer coefficient plotted as a function of coating thickness. The experimental results for the sputtered Teflon and Nedox coated specimens are also plotted in Figure 12.

2. C-6 Fluoroepoxy

For the machined specimens, the heat transfer coefficient increased as the coating thickness was reduced. The specimen with the 25 micron coating showed a reduction in the heat transfer coefficient when compared with the results of the uncoated specimen. The other two specimens showed only modest improvements in the heat transfer coefficient compared with filmwise. The uncertainty in coating thickness, and thermal conductivity, as well as the poor quality of dropwise condensation exhibited make the calculation of an expected heat transfer curve like that of Figure 12 impractical.

3. Nedox

The Nedox specimens with complete coatings (G3 and G4) gave excellent dropwise condensation. Specimen G1, which had a discontinuous coating gave good quality dropwise. Yet G1 and G3 showed only 10 and 20 percent improvements, respectively, in heat transfer coefficients over the uncoated specimen. Specimen G4 showed almost no improvement at all. If the additional resistances were due solely to one dimensional conduction through the Teflon layer, 0.2 to 0.6 microns thick,

an increase of over 300 percent would have been expected. Nedox had the additional conductive resistance through 3.0 to 10.0 microns of porous nickel. This is a difficult resistance to quantify. Pure nickel has a high thermal conductivity, 90 w/m^{o}C. The effective conductivity of the porous nickel, however, is unknown, and is probably different. It is believed that the resistance induced by the nickel coating was small compared with that induced by the Teflon coating. Also, the Teflon, nickel, and copper-nickel, all appeared to be well bonded, so contact resistance was considered to be negligible.

4. Sputtered Teflon

The sputtered Teflon was applied in ultra-thin coatings, 0.08 and 0.13 microns. As would be expected, these thinner coatings gave greater improvements in heat transfer than the thicker Nedox coatings. Thus, 58 and 47 percent improvements, respectively, in the heat transfer coefficient, were measured for the coated surfaces vs. the uncoated surface. Once again, the results were much lower than were predicted by the one dimensional conduction analysis.

5. Discussion of Coating Thickness Results

The heat transfer coefficient was found to increase with decreasing coating thickness. Even when the coating was discontinuous and the quality of dropwise condensation had deteriorated, an increase in heat transfer was still shown. There is probably a point (0.01 μm) where the coating becomes so discontinuous that it can no longer support dropwise condensation, and the heat transfer coefficient will start to decrease.

The data was surprising because the results were so much lower than expected. The one dimensional analysis used to generate the expected heat transfer curve was obviously not adequate to explain the experimental results. Three possible explanations of the results are presented here:

a. The discontinuous coatings gave dropwise condensation that was of slightly poorer quality than the chemically promoted surfaces. This could account for part of the difference between the experimental and expected results, but it is not considered adequate to explain the total difference.

b. The two specimens with continuous coatings (G3 and G4) both gave dropwise condensation as good as the chemically promoted specimens, yet they also showed a significantly lower heat transfer coefficient than expected. The porous nickel coating may have induced a significant resistance, but it does not seem probable.

c. It is known that Teflon will outgas to a very small degree when subjected to a vacuum. Even small quantities of non-condensables have been shown to significantly reduce the heat transfer coefficient of dropwise condensation [16]. It is possible that the condensing surface itself was acting as a source of non-condensables. The condensing vapor would tend to trap the gases close to the surface because the flow of the vapor is into the specimen. It is felt that this is probably the main cause of the difference between the expected and experimental values in heat transfer coefficient.

D. EFFECT OF NON-CONDENSABLES

Previous experimenters have shown non-condensable gases to have a devastating effect on the heat transfer during dropwise condensation. This experiment was no exception. The original experimental procedure used a bleed valve installed between the moisture separator and vacuum pump to control pressure in the chamber. Though this procedure allowed for very precise control of pressure, it also let air back into the condenser chamber. This caused a reduction in the heat transfer coefficient from 30 $kw/m^{2o}C$ to 8 $kw/m^{2o}C$. The thermal gradient within the specimen for the case with air present is not linear. It is thought that the reason for this non-linearity is that the air drawn to the condensing surface builds up, effectively insulating the condensing surface until blown away by a blast of steam from the boiler section. Visual observation of the specimen during dropwise condensation supports this theory. The dropwise condensation would periodically slow and almost stop; then it would start with what appeared to be a wave of steam over it.

Morgan [17] used a brush recorder to monitor the surface temperature of a specimen with dropwise condensation in the presence of non-condensables. He found that the surface temperature dropped $4^{o}C$ in a period of 2 seconds, and then rose $4^{o}C$ in the same period. This is the kind of temperature drop that would be expected from the accumulation of significant non-condensables on the surface, and the same kind of

a temperature variation that would give the results found in this experiment.

E. EFFECT OF CONDENSER MATERIAL

There was virtually no difference between the data for the copper and copper-nickel specimens. The chemically promoted copper specimen had a heat transfer coefficient of 143 $kw/m^{2o}C$. The similarly promoted copper-nickel specimen had a heat transfer coefficient of 138 $kw/m^{2o}C$. The copper and copper-nickel specimens with the 0.08 μm sputtered Teflon coatings had heat transfer coefficients of 36.5 and 35.5 $kw/m^{2o}C$ respectively. The Titanium specimen with the 0.08 μm sputtered Teflon coating had a heat transfer coefficient of 15.8 $kw/m^{2o}C$, which is significantly less than the values for the copper or copper-nickel.

F. EFFECT OF SURFACE ROUGHNESS

It was originally intended to determine the effect of surface roughness on the heat transfer coefficient. It was thought that having a smooth surface below the coating would tend to make the coating surface smoother. It was found that the Nedox and C-6 fluoroepoxy coatings were thick enough to smooth out any machining marks. The smooth and machined surfaces once coated had almost the same surface characteristics. Specimen N1, with a 15 μm thick coating of C-6 fluoroepoxy on a smooth surface gave slightly better performance than specimen N2, which had a 11 μm thick coating of C-6 fluoroepoxy. However, in light of the uncertainty in the heat transfer coefficient, and the uncertainty in the coating thickness, this difference

is not considered significant, and no conclusions can be drawn from this data on the effect of surface roughness on the heat transfer coefficient in dropwise condensation.

V. CONCLUSIONS

1. The organic polymers tested would not be acceptable permanent promoters of dropwise condensation. They only showed moderate improvements in heat transfer, and all showed signs of physical deterioration after very short operating periods.
2. The heat transfer coefficient was found to be a weak function of coating thickness. The increases were only moderate, ranging from -20 to 58 percent for the copper-nickel specimens. As coating thickness decreased, the difference between expected values and experimental values increased.
3. There is no significant change in the heat transfer coefficient between copper and copper-nickel. Titanium, however, does show a significant reduction in heat transfer coefficient compared to copper or copper-nickel.
4. The chemical promoter gave heat transfer coefficients five to six times those of the permanent coatings.
5. The presence of non-condensable gases causes a significant reduction in the heat transfer coefficient for dropwise condensation.

VI. RECOMMENDATIONS

1. Continue testing NRL fluoroepoxy coatings. It is believed that the fluoroepoxy may be modified to improve its physical characteristics for dropwise condensation [18]. It can be made more hydrophobic, or can be given higher thermal conductivity. Thinner coatings could also be used.
2. Explore the possibility that other permanent nonwetting coatings may be commercially available, both organic and metallic.
3. Conduct further tests with sputtered Teflon to obtain an ultra-thin continuous coating that will give better quality dropwise condensation.
4. Conduct analytical and experimental studies of outgassing of Teflon coated surfaces.
5. Build another experimental apparatus modeled after Graham [8]. The existing apparatus had several limitations. There was no way to measure vapor velocity past the specimen. The large nylon specimen holder, as well as the Teflon cup, probably induced non-condensables into the condensing chamber. Also, because of limitations of the cooling water system, the maximum heat flux through the specimen was around 80 $kw/m^{2o}C$. This was not adequate.

VII. TABLES

Specimen	Material	Coating	Nominal Thickness (microns)	Measured Thickness (microns)
N1	Cu-Ni	Fluoroepoxy	0.5	15 ± 5
N2	Cu-Ni	Fluoroepoxy	0.5	11 ± 5
N3	Cu-Ni	Fluoroepoxy	2.0	16 ± 5
N4	Cu-Ni	Fluoroepoxy	5.0	25 ± 5
G1	Cu-Ni	Nedox	3.0 Total (0.3-0.5 Teflon)	3.0 Total (0.2 ±0.2 Teflon)
G3	Cu-Ni	Nedox	5.0 Total (0.3-0.5 Teflon)	5.0 Total (0.4 ±0.2 Teflon)
G4	Cu-Ni	Nedox	10.0 Total (0.3-0.5 Teflon)	10.0 Total (0.6 ±0.2 Teflon)
T1	Cu-Ni	Sputtered Teflon	0.08	-
T2	Cu-Ni	Sputtered Teflon	0.13	-
T3	Copper	Sputtered Teflon	0.08	-
T4	Titanium	Sputtered Teflon	0.08	-
C1	Cu-Ni	Chemically Promoted	-	-
C2	Copper	Chemically Promoted	-	-
X	Cu-Ni	Uncoated	-	-

Table I. Summary of Specimens Tested

Specimen	Material	Coating	Coating Thickness (microns)	Dropwise Performance	$\frac{h}{h_{un}}$	$\frac{h}{(kw/m^2 {}^oC)}$
N1	Cu-Ni	Fluoroepoxy	15	Fair	1.38	31.0
N2	Cu-Ni	Fluoroepoxy	11	Poor	1.31	29.5
N3	Cu-Ni	Fluoroepoxy	16	Fair	1.20	27.0
N4	Cu-Ni	Fluoroepoxy	25	Poor	0.80	17.9
G1	Cu-Ni	Nedox	3 (Total) 0.2 Teflon	Good	1.18	26.5
G3	Cu-Ni	Nedox	5 (Total) 0.4 Teflon	Excellent	1.28	28.9
G4	Cu-Ni	Nedox	10 (Total) 0.6 Teflon	Excellent	1.07	24.0
T1	Cu-Ni	Sputtered Teflon	0.08	Good	1.58	35.5
T2	Cu-Ni	Sputtered Teflon	0.13	Good	1.47	35.0
T3	Copper	Sputtered Teflon	0.08	Good	1.61	36.5
T4	Titanium	Sputtered Teflon	0.08	Good	0.70	15.8

Continued

Table II. Summary of Heat Transfer Results

Specimen	Material	Coating	Coating Thickness (microns)	Dropwise Performance	$\frac{h}{h_{un}}$	$\frac{h}{(kw/m^{2o}C)}$
C1	Cu-Ni	Chemically Promoted	-	Excellent	6.13	138
C2	Copper	Chemically Promoted	-	Excellent	6.36	143
X	Cu-Ni	Uncoated	-	Filmwise	1.0	22.5

Table II. (Cont'd)

Thermophysical Properties

1. Thermal Conductivity

Material	k (w/m°C)	Source
90-10 Cu-Ni	56	GE Heat Transfer Handbook [22]
Copper	384	Tolukian [23]
Titanium	20	Tolukian
Teflon	.170	GE Heat Transfer Handbook
Epoxy	.198	GE Heat Transfer Handbook

2. Physical Properties of Water at 60°C

h_{fg}	2.36×10^6 J/kg	Reynolds & Perkins [25]
ρ	983.2 kg/m	Reynolds & Perkins
μ	5.13×10^{-4} kg/m·s	Holman [24]
k	0.654 w/m °C	Holman

Table III. Thermophysical Properties of Pertinent Materials

Data Pt.	Thermocouple Location							
	1	2	3	4	5	6	T_v	
1.	50.65	52.64	54.26	55.76	57.36	57.31	59.58	(^oC)
	2.071	2.152	2.223	2.279	2.342	2.335	2.420	(mv)
2.	46.96	49.06	51.26	53.66	56.33	56.22	59.49	
	1.909	1.999	2.096	2.190	2.298	2.290	2.416	
3.	45.63	48.11	50.62	52.92	55.74	55.62	59.32	
	1.851	1.957	2.069	2.159	2.273	2.265	2.409	
4.	44.67	47.29	49.79	52.62	55.45	55.29	55.43	
	1.811	1.920	2.033	2.146	2.261	2.251	2.415	
5.	42.35	45.70	48.67	51.71	55.19	54.58	59.60	
	1.719	1.850	1.983	2.108	2.250	2.221	2.421	
6.	40.68	44.27	47.73	50.75	54.34	54.17	59.53	
	1.653	1.791	1.940	2.067	2.215	2.204	2.418	

	Data Pt.						
	1	2	3	4	5	6	
T_s	58.88	58.41	58.04	57.97	57.98	57.64	(^oC)
ΔT	0.70	1.07	1.26	1.49	1.61	1.89	(^oC)
Q/A	34.3	51.2	54.8	58.9	68.5	74.2	(kw/m^2)
h	48.9	47.5	42.8	39.5	42.5	39.2	($kw/m^{2o}C$)

Table IV. Data for Tl, Sputtered Teflon, 0.08 μm Coating on Cu-Ni

Data Pt.	Thermocouple Location 1	2	3	4	5	6	T_v	
1.	50.88	52.59	54.26	55.69	57.13	56.90	59.51	(^oC)
	2.081	2.150	2.223	2.276	2.332	2.318	2.417	(mv)
2.	49.05	51.29	53.41	54.89	56.75	56.29	59.53	
	2.002	2.095	2.187	2.242	2.316	2.293	2.418	
3.	48.13	50.46	52.79	54.51	56.30	56.10	59.77	
	1.961	2.060	2.161	2.226	2.297	2.285	2.428	
4.	44.81	47.62	50.16	52.73	55.27	54.89	59.35	
	1.817	1.935	2.049	2.151	2.253	2.234	2.410	
5.	42.23	45.72	48.80	51.50	54.46	54.08	59.51	
	1.714	1.851	1.989	2.099	2.219	2.200	2.417	
6.	39.63	43.66	47.42	50.20	53.34	53.04	59.18	
	1.610	1.767	1.926	2.044	2.172	2.156	2.403	

	Data Pt. 1	2	3	4	5	6	
T_s	58.79	58.59	58.47	57.78	57.46	56.92	(^oC)
ΔT	0.72	0.94	1.30	1.56	2.05	2.26	(^oC)
Q/A	34.4	40.9	44.4	56.6	65.8	74.2	(kw/m^2)
h	47.8	43.5	34.1	35.9	32.1	32.8	($kw/m^{2o}C$)

Table V. Data for T2, Sputtered Teflon, 0.13 μm Coating on Cu-Ni

Data Pt.	Thermocouple Location							
	1	2	3	4	5	6	T_v	
1.	58.32	58.48	58.58	58.81	58.96	58.99	59.58	(^oC)
	2.397	2.401	2.409	2.407	2.410	2.405	2.420	(mv)
2.	57.78	58.01	58.17	58.43	58.61	58.73	59.53	
	2.374	2.381	2.391	2.391	2.395	2.394	2.418	
3.	56.89	57.32	57.63	57.95	58.23	58.24	59.72	
	2.336	2.351	2.368	2.371	2.379	2.374	2.426	
4.	56.06	56.48	56.82	57.24	57.69	57.69	59.67	
	2.301	2.315	2.333	2.341	2.356	2.351	2.424	
5.	55.03	55.62	56.01	56.43	56.92	56.90	59.25	
	2.257	2.278	2.298	2.307	2.323	2.318	2.406	

	Data Pt.					
	1	2	3	4	5	
T_s	59.12	58.89	58.61	58.06	57.38	(^oC)
ΔT	0.46	0.64	1.12	1.61	1.87	(^oC)
Q/A	24.6	33.7	50.3	60.8	69.4	(kw/m^2)
h	53.7	52.4	45.2	37.7	37.1	($kw/m^{2o}C$)

Table VI. Data for T3, Sputtered Teflon 0.08 μm Coating on Copper

Data Pt.	Thermocouple Location						
	1	2	3	4	5	6	T_v
1.	-	48.90	51.35	53.99	56.54	56.30	59.44 (^oC)
	-	1.992	2.100	2.204	2.307	2.293	2.414 (mv)
2.	-	47.49	50.44	53.39	56.12	56.01	59.70
	-	1.929	2.061	2.179	2.289	2.264	2.425
3.	-	47.57	49.40	52.71	55.76	55.72	59.88
	-	1.888	2.016	2.150	2.274	2.269	2.433
4.	-	45.65	48.71	52.16	55.38	44.48	59.88
	-	1.848	1.985	2.127	2.258	2.259	2.433
5.	-	41.79	45.76	49.85	53.94	54.03	59.74
	-	1.695	1.852	2.029	2.197	2.198	2.427

	Data Pt.					
	1	2	3	4	5	
T_s	59.04	59.01	58.81	58.61	57.89	(^oC)
ΔT	0.39	0.69	1.07	1.28	1.85	(^oC)
Q/A	20.0	22.6	24.3	25.6	31.7	(kw/m^2)
h	51.4	32.7	22.7	20.1	17.2	($kw/m^{2o}C$)

Table VII. Data for T4, Sputtered Teflon 0.08 μm Coating on Titanium

Data Pt.	Thermocouple Location							
	1	2	3	4	5	6	T_v	
1.	53.76	54.89	55.82	56.64	57.72	57.69	59.18	(^oC)
	2.203	2.247	2.290	2.316	2.357	2.351	2.403	(mv)
2.	49.08	51.38	52.84	54.46	56.30	56.32	59.11	
	2.003	2.099	2.163	2.224	2.297	2.294	2.400	
3.	48.98	51.36	52.77	54.34	56.19	56.15	59.09	
	1.999	1.098	2.160	2.219	2.292	2.287	2.399	
4.	49.85	51.95	53.36	54.58	56.49	56.34	59.23	
	2.037	2.123	2.185	2.229	2.305	2.295	2.405	
5.	44.07	47.42	49.38	51.71	54.67	54.67	59.16	
	1.787	1.926	2.015	2.108	2.228	2.225	2.402	
6.	44.02	47.49	49.43	51.62	54.39	54.62	59.16	
	1.785	1.929	2.017	2.104	2.216	2.223	2.402	

	Data Pt.						
	1	2	3	4	5	6	
T_s	58.66	58.08	57.93	57.95	57.10	56.94	(^oC)
ΔT	0.52	1.03	1.16	1.27	2.06	2.22	(^oC)
Q/A	21.3	38.6	38.3	34.7	56.2	55.3	(kw/m^2)
h	40.9	37.4	33.1	27.4	27.3	25.0	($kw/m^{2o}C$)

Table VIII. Data for Gl, Nedox, 3.0 μm Coating on Cu-Ni

Data Pt.	Thermocouple Location							
	1	2	3	4	5	6	T_v	
1.	53.45	54.72	55.57	56.64	57.67	57.69	59.18	(^oC)
	2.190	2.240	2.279	2.316	2.355	2.351	2.403	(mv)
2.	51.26	52.88	54.00	55.43	56.73	56.82	58.97	
	2.097	2.162	2.212	2.265	2.315	2.315	2.394	
3.	51.28	52.83	54.00	55.46	56.80	56.85	58.97	
	2.098	2.160	2.212	2.266	2.318	2.316	2.394	
4.	47.57	49.9	51.52	53.58	55.58	55.64	59.13	
	1.936	2.036	2.107	2.187	2.269	2.268	2.401	
5.	47.52	50.06	51.61	54.20	56.61	56.80	60.52	
	1.934	2.043	2.111	2.313	2.310	2.314	2.460	
6.	43.70	46.77	49.00	51.67	54.53	54.25	58.99	
	1.772	1.897	1.998	2.106	2.222	2.207	2.395	

	Data Pt.						
	1	2	3	4	5	6	
T_s	58.73	58.18	58.20	57.65	59.07	56.99	(^oC)
ΔT	0.45	0.79	0.77	1.51	1.63	2.00	(^oC)
Q/A	22.9	30.2	30.3	43.7	49.9	57.9	(kw/m^2)
h	50.4	38.1	39.2	28.9	30.6	29.0	($kw/m^{2o}C$)

Table IX. Data for G3, Nedox, 50 μm Coating on Cu-Ni

Data Pt.	Thermocouple Location							
	1	2	3	4	5	6	T_v	
1.	52.67	53.73	54.96	56.26	57.39	57.40	59.18	(^oC)
	2.157	2.198	2.253	2.300	2.343	2.339	2.403	(mw)
2.	50.25	51.69	53.29	55.03	56.68	56.70	59.13	
	2.054	2.112	2.182	2.248	2.248	2.313	2.401	
3.	49.49	50.98	52.70	54.53	56.28	56.41	59.13	
	2.021	2.082	2.157	2.227	2.296	2.298	2.401	
4.	47.93	49.58	51.47	53.61	55.74	55.79	59.13	
	1.952	2.022	2.105	2.188	2.273	2.272	2.401	
5.	46.46	48.03	49.90	52.64	55.17	55.20	59.13	
	1.887	1.953	2.038	2.147	2.249	2.247	2.401	
6.	45.30	46.98	48.98	51.95	54.77	54.89	59.09	
	1.837	1.906	1.997	2.118	2.232	2.234	2.399	

	Data Pt.						
	1	2	3	4	5	6	
T_s	58.60	58.26	57.99	57.58	57.07	56.83	(^oC)
ΔT	0.58	0.87	1.14	1.55	2.07	2.27	(^oC)
Q/A	26.4	35.8	38.0	43.4	48.7	53.0	(kw/m^2)
h	45.6	40.9	33.4	28.0	23.6	23.4	($kw/m^{2o}C$)

Table X. Data for G4, Nedox, 10 μm Coating on Cu-Ni

Data Pt.	Thermocouple Location							
	1	2	3	4	5	6	T_v	
1.	51.52	52.90	54.59	55.91	57.10	56.97	59.09	(^oC)
	2.108	2.163	2.237	2.285	2.331	2.321	2.399	(mv)
2.	50.09	51.62	53.74	55.55	56.87	56.82	59.35	
	2.047	2.109	2.201	2.270	2.321	2.315	2.410	
3.	47.99	49.53	51.83	54.34	56.14	55.94	59.16	
	1.955	2.020	2.120	2.219	2.290	2.278	2.402	
4.	45.46	47.51	50.39	53.18	55.22	55.10	59.25	
	1.844	1.930	2.059	2.170	2.251	2.243	2.406	
5.	44.86	47.02	50.02	52.76	54.56	54.27	59.25	
	1.819	1.908	2.043	2.152	2.223	2.208	2.406	

	Data Pt.					
	1	2	3	4	5	
T_s	58.60	58.80	58.22	57.86	57.54	(^oC)
ΔT	0.49	0.55	0.94	1.39	1.71	(^oC)
Q/A	31.0	38.5	46.1	55.3	57.1	(kw/m^2)
h	63.6	69.9	49.0	39.8	33.4	($kw/m^{2o}C$)

Table XI. Data for Nl, C-6 Fluoroepoxy, 16 μm Coating on Cu-Ni

Data Pt.	Thermocouple Location							
	1	2	3	4	5	6	T_v	
1.	51.26	52.73	54.35	55.65	57.03	57.11	59.39	(^oC)
	2.097	2.156	2.227	2.274	2.328	2.327	2.412	(mv)
2.	49.74	51.45	53.43	54.96	56.49	56.27	59.16	
	2.032	2.102	2.188	2.245	2.305	2.292	2.402	
3.	48.11	50.06	52.37	54.20	56.26	56.15	59.18	
	1.960	2.043	2.143	2.213	2.295	2.287	2.403	
4.	46.32	48.45	50.93	53.04	55.41	55.34	59.27	
	1.881	1.972	2.082	2.164	2.259	2.253	2.407	
5.	45.39	47.56	50.09	52.35	54.98	54.93	59.13	
	1.841	1.932	2.046	2.135	2.241	2.236	2.401	

	Data Pt.					
	1	2	3	4	5	
T_s	58.57	58.23	58.28	57.66	57.25	(^oC)
ΔT	0.82	0.93	0.90	1.61	1.88	(^oC)
Q/A	32.1	37.0	44.8	50.2	52.8	(kw/m^2)
h	39.3	39.8	50.0	31.2	28.0	($kw/m^{2o}C$)

Table XII. Data for N2, C-6 Fluoroepoxy, 11 μm Coating on Cu-Ni

Data Pt.	Thermocouple Location							
	1	2	3	4	5	6	T_v	
1.	52.72	53.85	54.94	56.05	56.96	56.78	59.27	(^oC)
	2.159	2.203	2.252	2.291	2.325	2.313	2.407	(mv)
2.	50.44	52.12	53.57	54.86	56.33	55.89	59.32	
	2.062	2.130	2.194	2.241	2.298	2.276	2.408	
3.	49.51	51.22	52.72	54.37	56.12	55.79	59.37	
	2.022	2.092	2.158	2.220	2.289	2.272	2.411	
4.	46.30	48.38	50.37	52.45	54.56	54.17	59.27	
	1.880	1.969	2.058	2.139	2.223	2.204	2.407	
5.	45.53	47.85	49.99	52.28	54.56	53.89	59.35	
	1.847	1.945	1.042	2.132	2.223	2.192	2.410	
6.	43.62	46.30	48.71	50.86	53.46	53.08	59.25	
	1.769	1.876	1.985	2.072	2.177	2.158	2.406	

	Data Pt.						
	1	2	3	4	5	6	
T_s	58.08	57.82	57.70	56.59	56.52	55.71	(^oC)
ΔT	1.19	1.5	1.67	2.68	2.83	3.54	(^oC)
Q/A	23.4	32.0	36.1	45.4	48.1	52.6	(kw/m^2)
h	19.6	21.3	21.6	16.9	17.0	14.9	($kw/m^{2o}C$)

Table XIII. Data for N3, C-6 Fluoroepoxy, 25 μm Coating on Cu-Ni

Data Pt.	Thermocouple Location						
	1	2	3	4	5	6	T_v
1.	52.79	53.99	55.29	56.31	57.36	57.23	59.37 (^oC)
	2.162	2.209	2.267	2.302	2.342	2.332	2.411 (mw)
2.	50.51	52.16	53.83	55.22	56.66	56.32	59.37
	2.065	2.132	2.205	2.256	2.312	2.294	2.411
3.	49.03	50.86	52.84	54.46	56.23	55.94	59.44
	2.001	2.077	2.163	2.224	2.294	2.278	2.414
4.	47.34	49.60	51.61	53.68	55.55	55.17	59.30
	1.926	2.023	2.111	2.191	2.265	2.246	2.408
5.	46.55	48.81	50.86	53.23	55.45	55.10	59.32
	1.891	1.988	2.079	2.172	2.261	2.243	2.409
6.	43.60	46.48	48.87	51.48	54.03	53.68	58.78
	1.768	1.884	1.992	2.098	2.201	2.183	2.386

	Data Pt.						
	1	2	3	4	5	6	
T_s	58.53	58.15	57.97	57.55	57.51	56.51	(^oC)
ΔT	0.84	1.22	1.47	1.74	1.81	2.27	(^oC)
Q/A	25.0	33.1	39.0	44.4	49.2	56.2	(kw/m^2)
h	29.9	27.1	26.5	25.4	26.6	24.8	($kw/m^{2o}C$)

Table XIV. Data for N4, C-6 Fluoroepoxy, 15 μm Coating on Cu-Ni

Data Pt.	Thermocouple Location							
	1	2	3	4	5	6	T_v	
1.	-	43.43	-	51.86	55.90	55.48	60.42	(^oC)
	-	1.758	-	2.114	2.280	2.259	2.456	(mv)
2.	-	45.84	-	52.94	56.37	55.98	60.26	
	-	1.856	-	2.160	2.300	2.280	2.449	
3.	-	42.83	-	51.38	55.62	55.29	60.35	
	-	1.735	-	2.094	2.268	2.251	2.435	
4.	-	47.02	-	53.49	56.66	56.29	60.33	
	-	1.908	-	2.183	2.312	2.293	2.452	
5.	-	46.84	-	53.28	56.45	56.13	60.14	
	-	1.900	-	2.174	2.303	2.286	2.444	

	Data Pt.					
	1	2	3	4	5	
T_s	59.91	59.73	59.73	59.71	59.51	(^oC)
ΔT	0.52	0.54	0.62	0.62	0.63	(^oC)
Q/A	90.5	76.3	93.0	69.7	69.7	(kw/m^2)
h	176.0	142.0	149.0	112.0	110.0	($kw/m^{2o}C$)

Table XV. Data for C1, Chemically Promoted 90-10 Cu-Ni.

Data Pt.	Thermocouple Location						
	1	2	3	4	5	6	T_v
1.	-	55.87	56.61	57.19	57.93	57.91	59.30 (^oC)
	-	2.289	2.324	2.339	2.366	2.360	2.408 (mv)
2.	-	55.29	56.22	56.98	57.97	57.88	59.63
	-	2.264	2.307	2.330	2.368	2.359	2.422
3.	-	56.81	57.52	58.12	58.82	58.75	60.00
	-	2.329	2.363	2.378	2.404	2.395	2.438
4.	-	56.83	57.59	58.10	58.89	58.73	60.19
	-	2.330	2.366	2.377	2.407	2.394	2.446

	Data Pt.				
	1	2	3	4	
T_s	58.58	58.73	59.45	59.37	(^oC)
ΔT	0.72	0.90	0.56	0.83	(^oC)
Q/A	101.7	128.9	98.8	93.8	(kw/m^2)
h	141.0	142.5	178.0	113.8	($kw/m^{2o}C$)

Table XVI. Data for C2, Chemically Promoted Copper.

Data Pt.	Thermocouple Location						
	1	2	3	4	5	6	T_v
1.	-	55.19	56.33	57.41	58.35	58.27	59.81 (^oC)
	-	2.260	2.312	2.348	2.384	2.375	2.430 (mv)
2.	-	53.54	55.22	56.43	57.62	57.52	59.74
	-	2.190	2.264	2.307	2.353	2.344	2.427
3.	-	51.62	53.22	55.27	56.82	56.83	59.84
	-	2.109	2.179	2.258	2.319	2.303	2.431
4.	-	49.88	52.32	54.15	55.97	55.67	59.56
	-	2.035	2.141	2.211	2.283	2.267	2.419
5.	-	48.61	51.21	53.21	55.41	55.08	59.88
	-	1.979	2.094	2.171	2.259	2.242	2.433
6.	-	45.95	48.89	51.27	53.91	53.49	59.56
	-	1.861	1.993	2.089	2.196	2.175	2.419

	Data Pt.						
	1	2	3	4	5	6	
T_s	59.38	58.97	58.36	57.81	57.38	56.15	(^oC)
ΔT	0.43	0.78	1.48	1.75	2.50	3.41	(^oC)
Q/A	22.8	29.0	37.0	42.3	47.2	55.1	(kw/m^2)
h	52.9	37.4	24.9	24.2	18.9	16.2	($kw/m^{2o}C$)

Table XVII. Data for the Uncoated Cu-Ni Specimen, Filmwise.

Specimen	Q/A Condensate flow rate (kw/m^2)	Q/A Fourier's law (kw/m^2)	Percent difference
C1	107.8	90.5	-16
C1	98.9	76.3	-22
C1	103.3	93.0	-8
C2	101.6	98.9	-3
G3	95.9	74.2	-22
N1	60.8	55.1	-9
T1	67.5	69.4	+3
T3	57.5	57.1	-1
X	51.9	57.9	+10

Table XVIII. Comparision of Heat Flux Data from Thermal Gradient and Condensate Flow Rate Data.

VIII. FIGURES

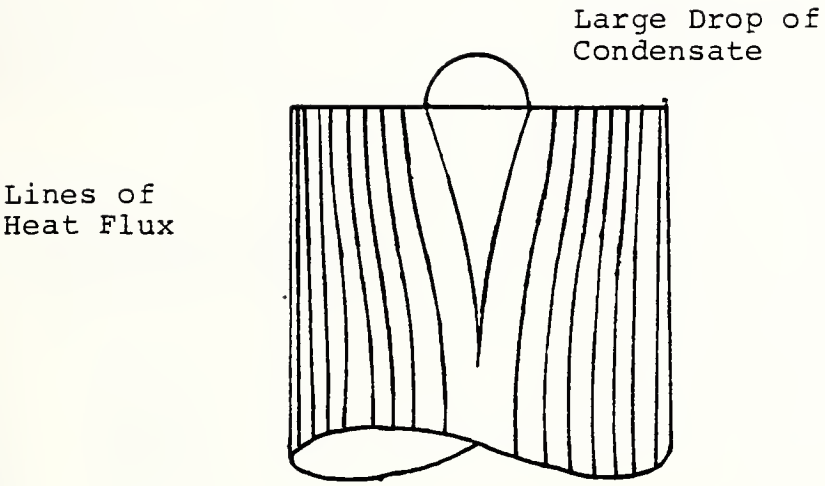

Figure 1. Visualization of Heat Flux Near Surface Due to Dropwise Condensation.

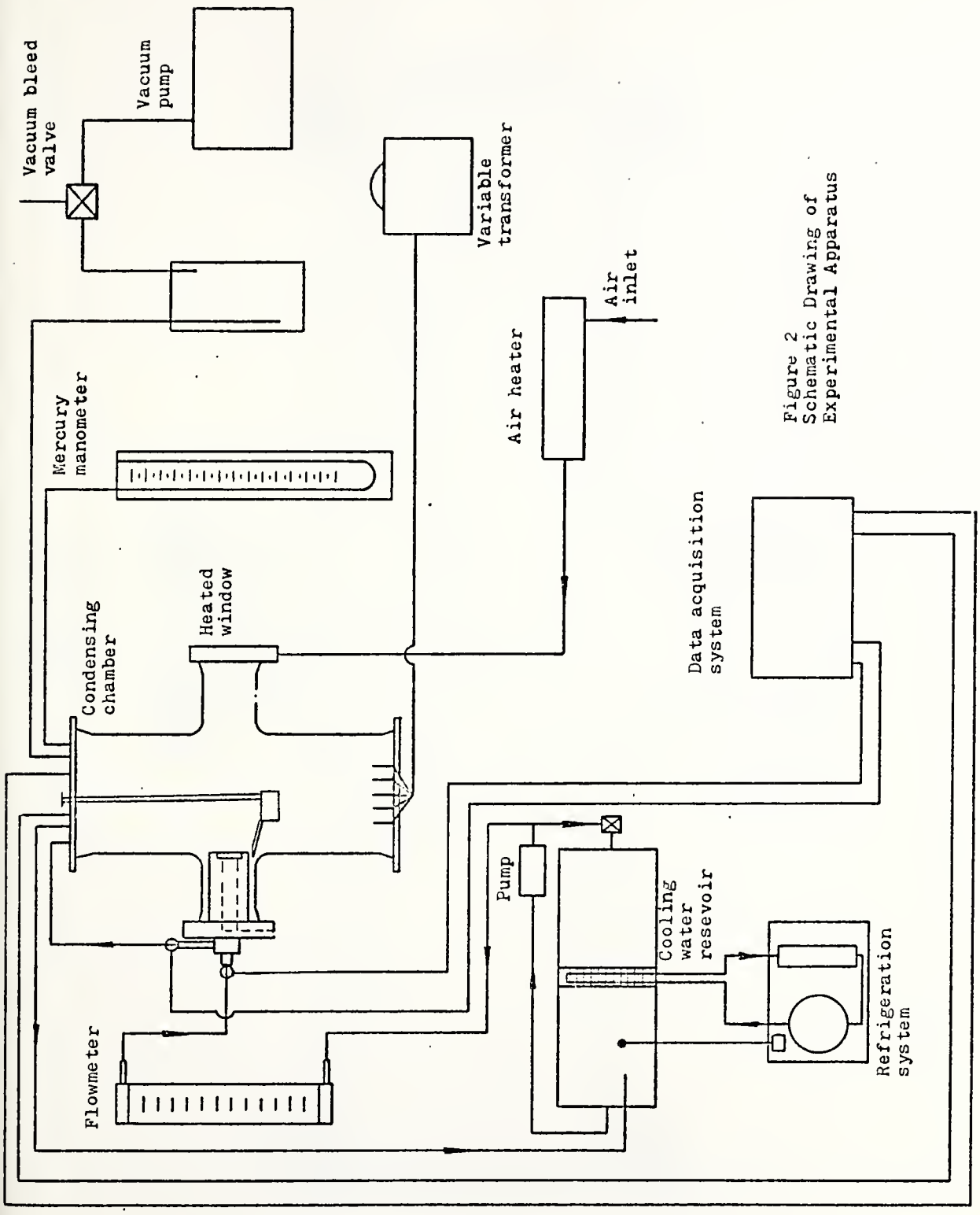

Figure 2 Schematic Drawing of Experimental Apparatus

Figure 2. Schematic Drawing of Experimental Apparatus

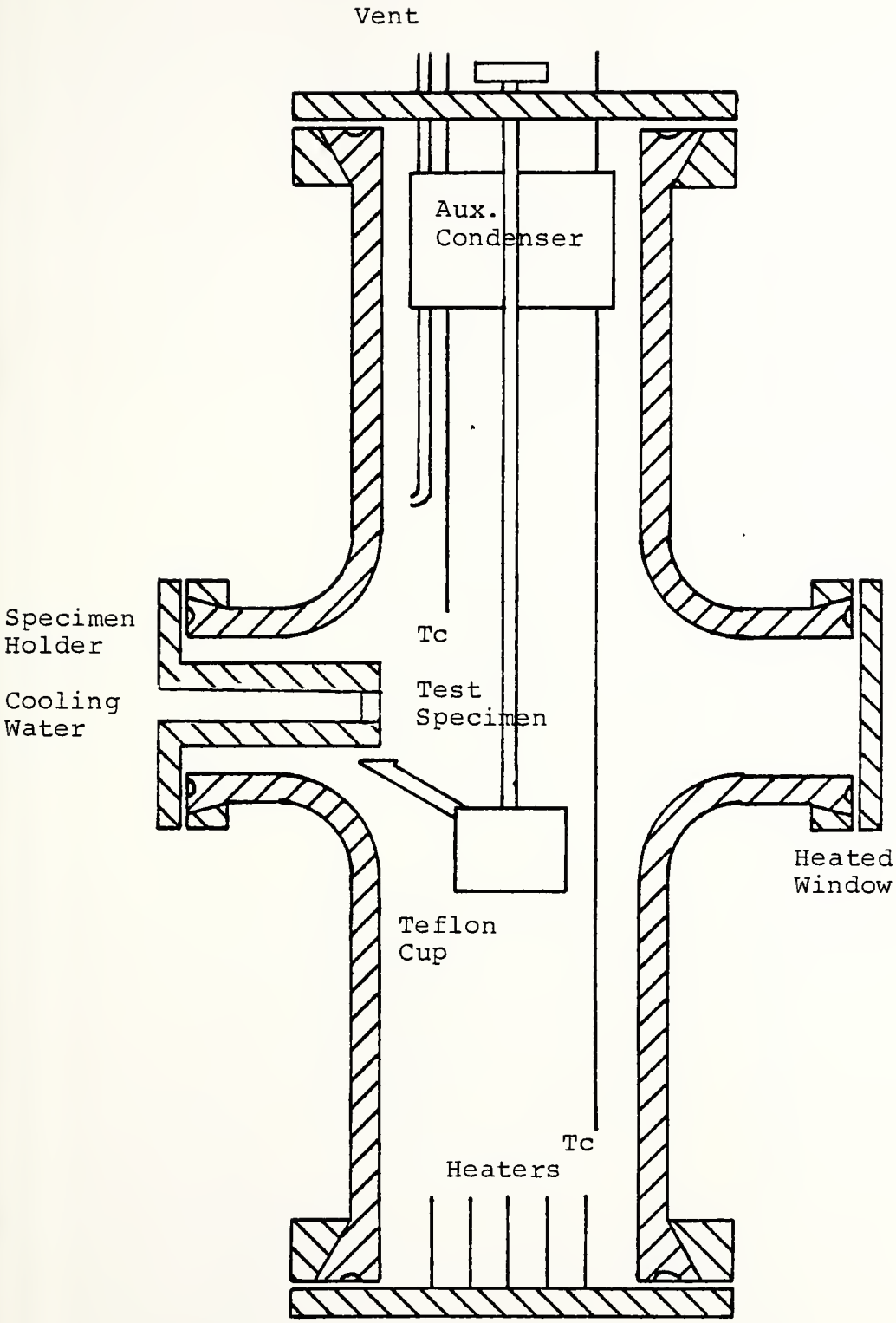

Figure 3. Condensing Chamber

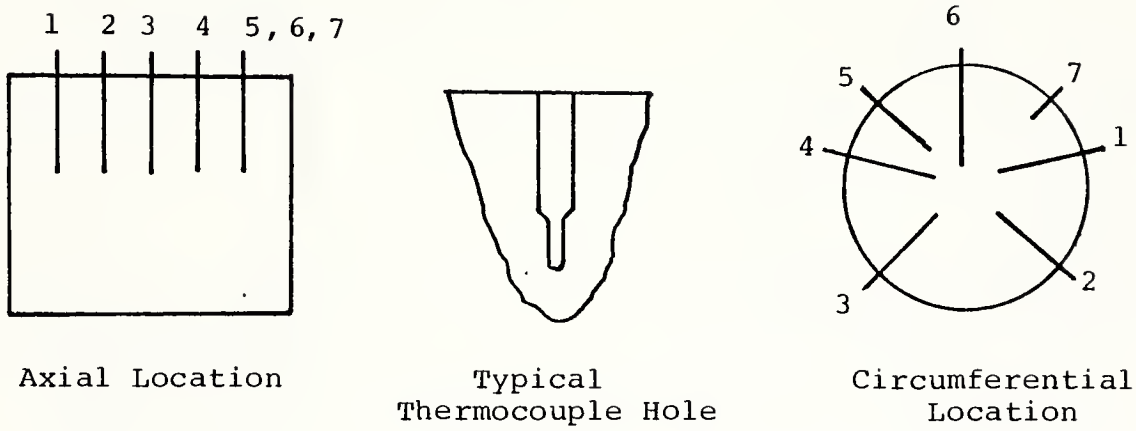

Figure 4. Thermocouple Hole Locations and a Typical Thermocouple Hole.

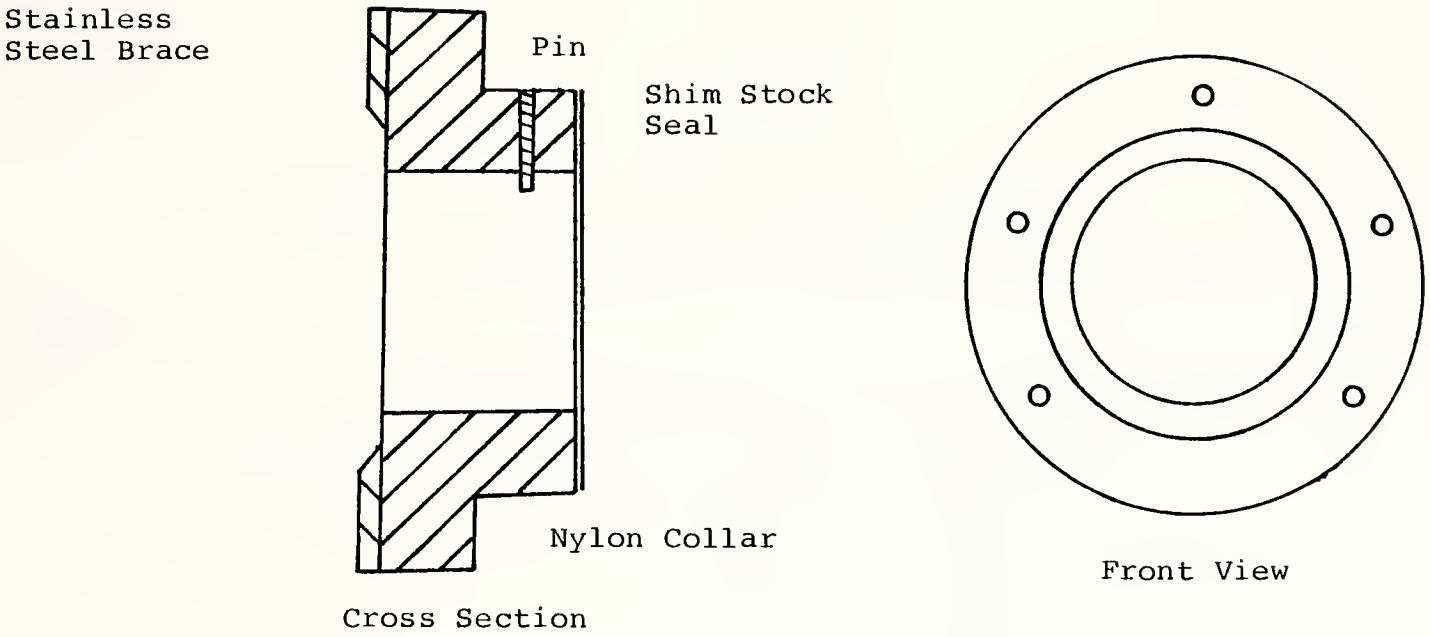

Figure 5. Nylon Retainer Ring

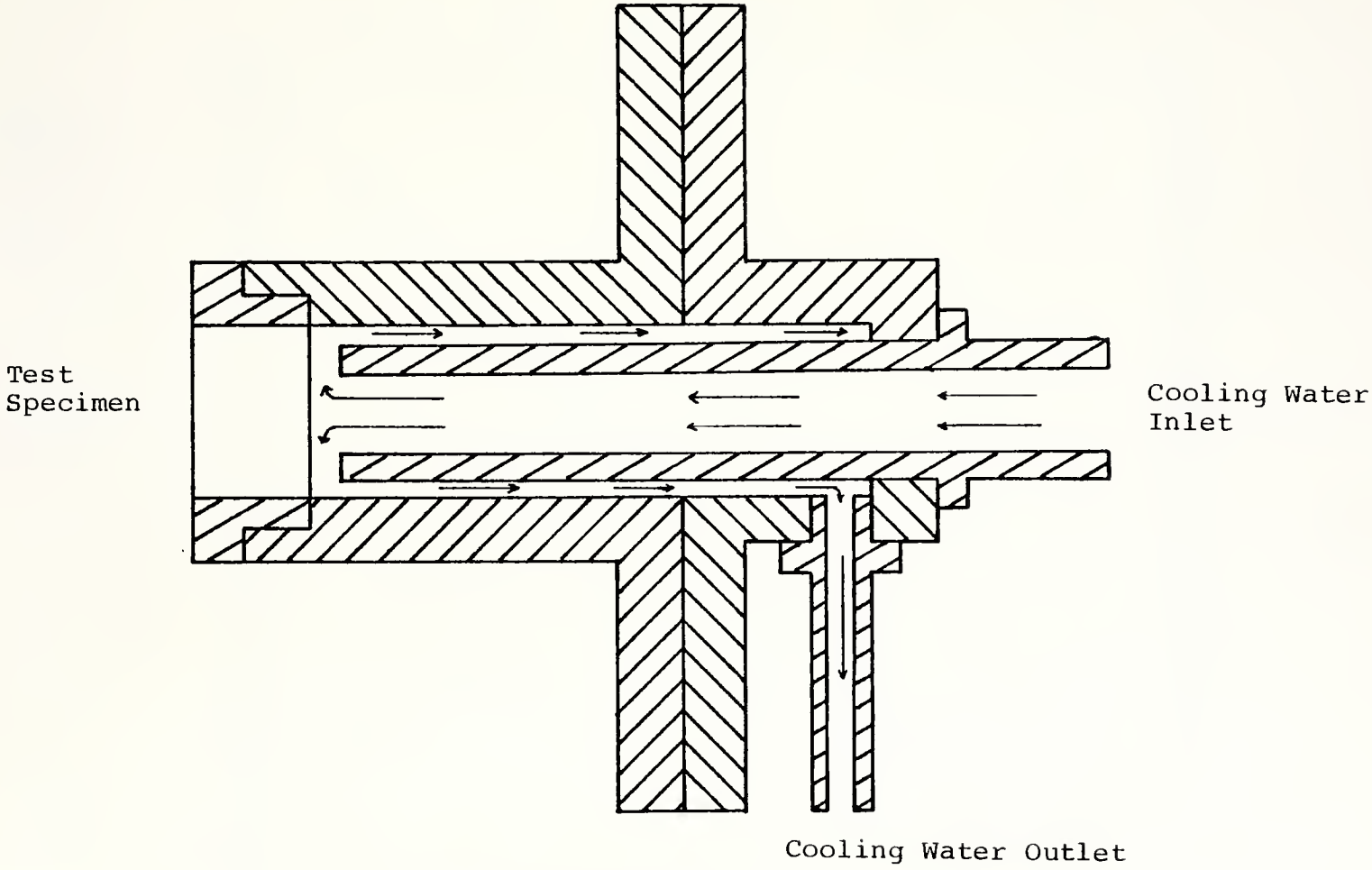

Figure 6. Specimen Holder

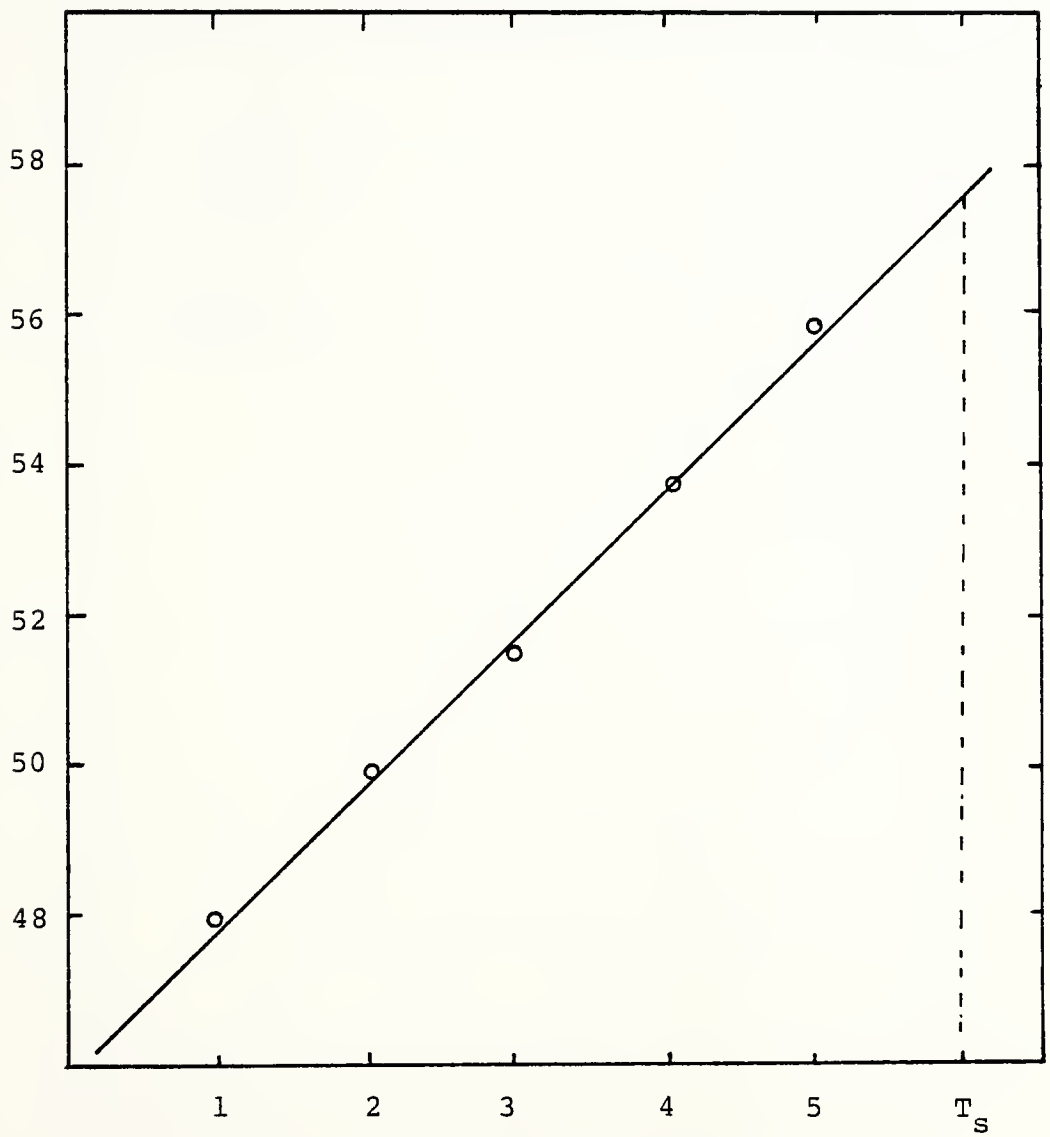

Figure 7. Typical Thermal Gradient. G4, Nedox, 7 Oct 79
$\Delta T = 1.55^{o}C$.

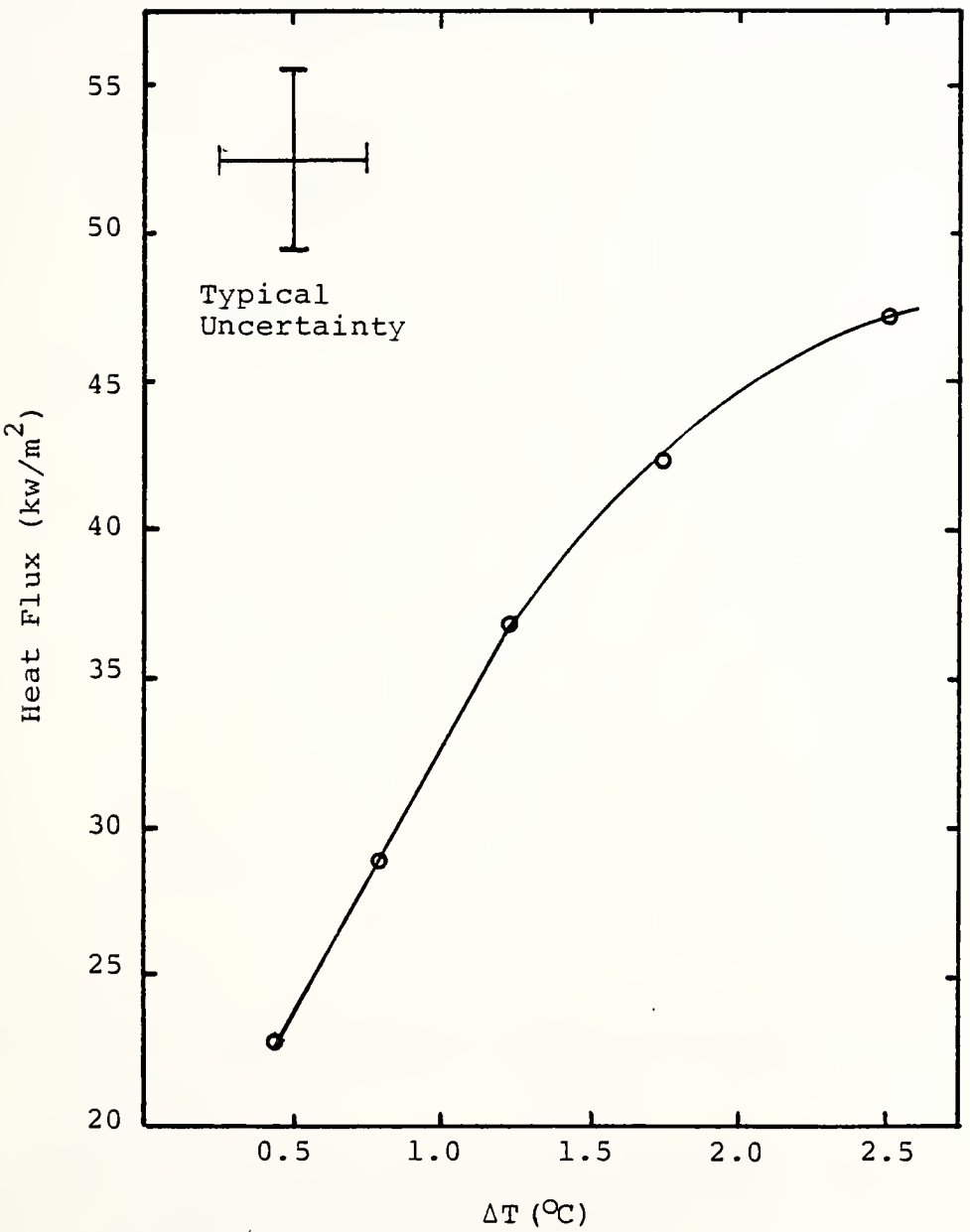

Figure 8. Heat Flux vs. ΔT for the Uncoated Copper-Nickel Specimen, Filmwise Condensation.

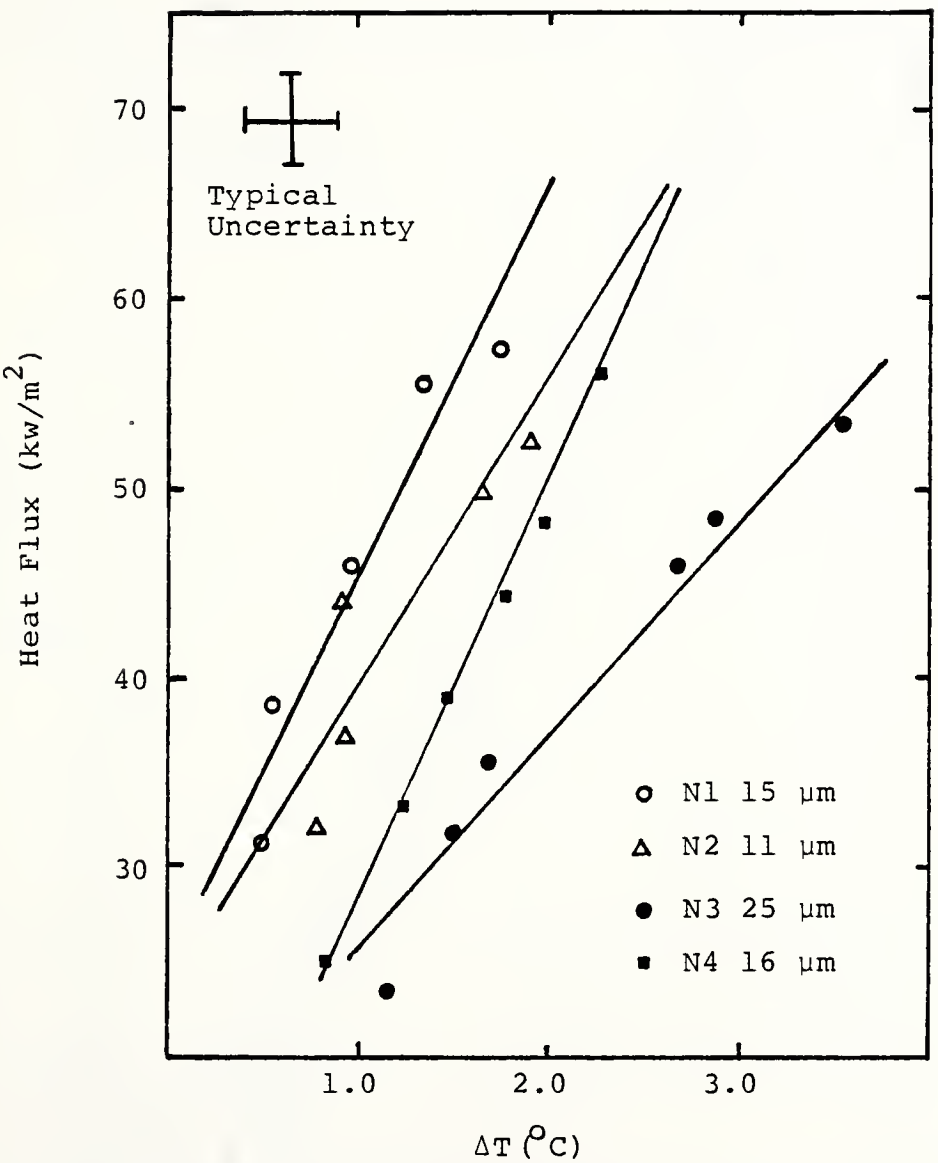

Figure 9. Heat Flux vs. ΔT for the C-6 Fluoroepoxy Coatings on Copper-Nickel Specimens

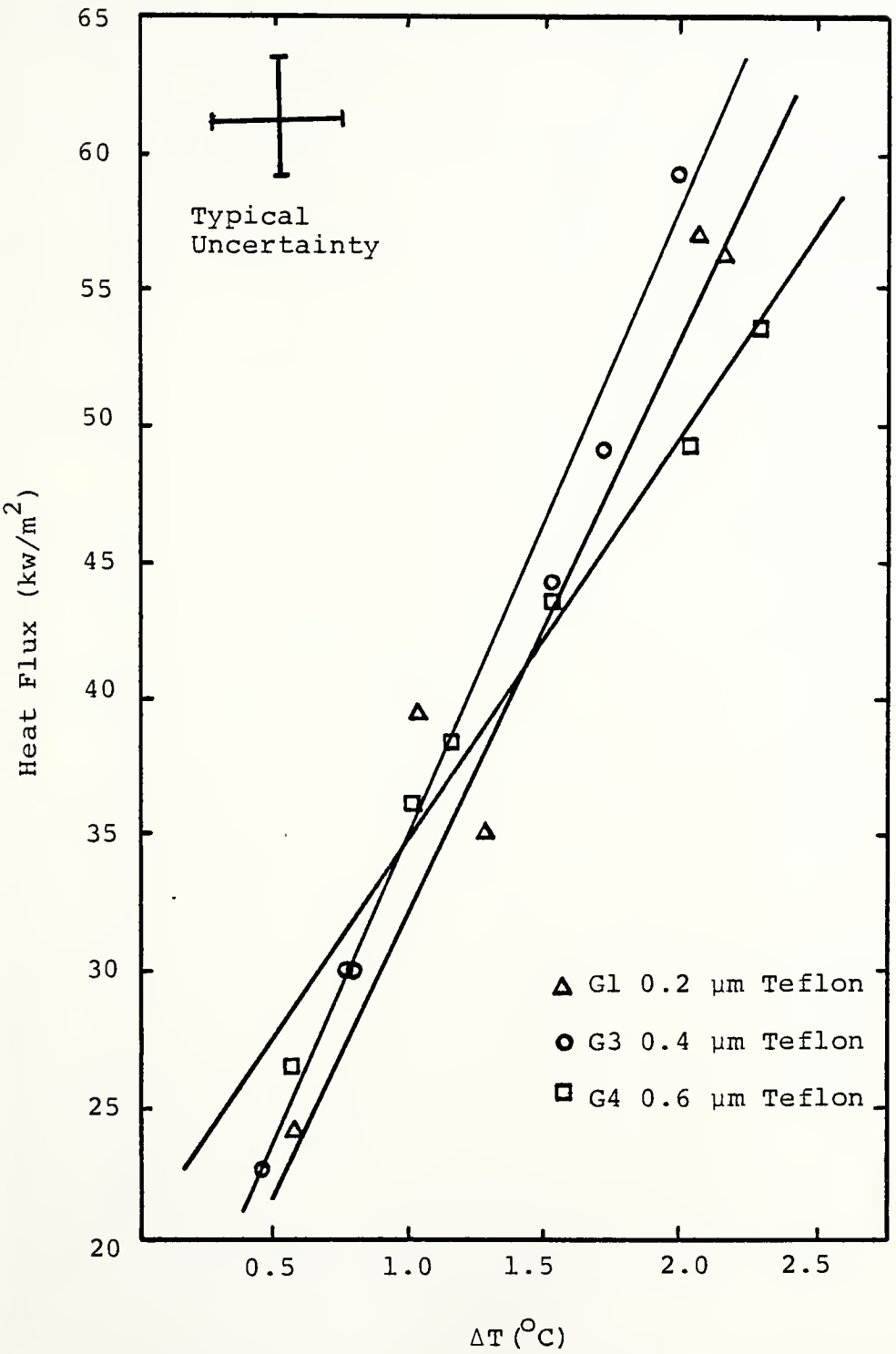

Figure 10. Heat Flux vs. ΔT for Nedox Coatings on Copper-Nickel Specimens.

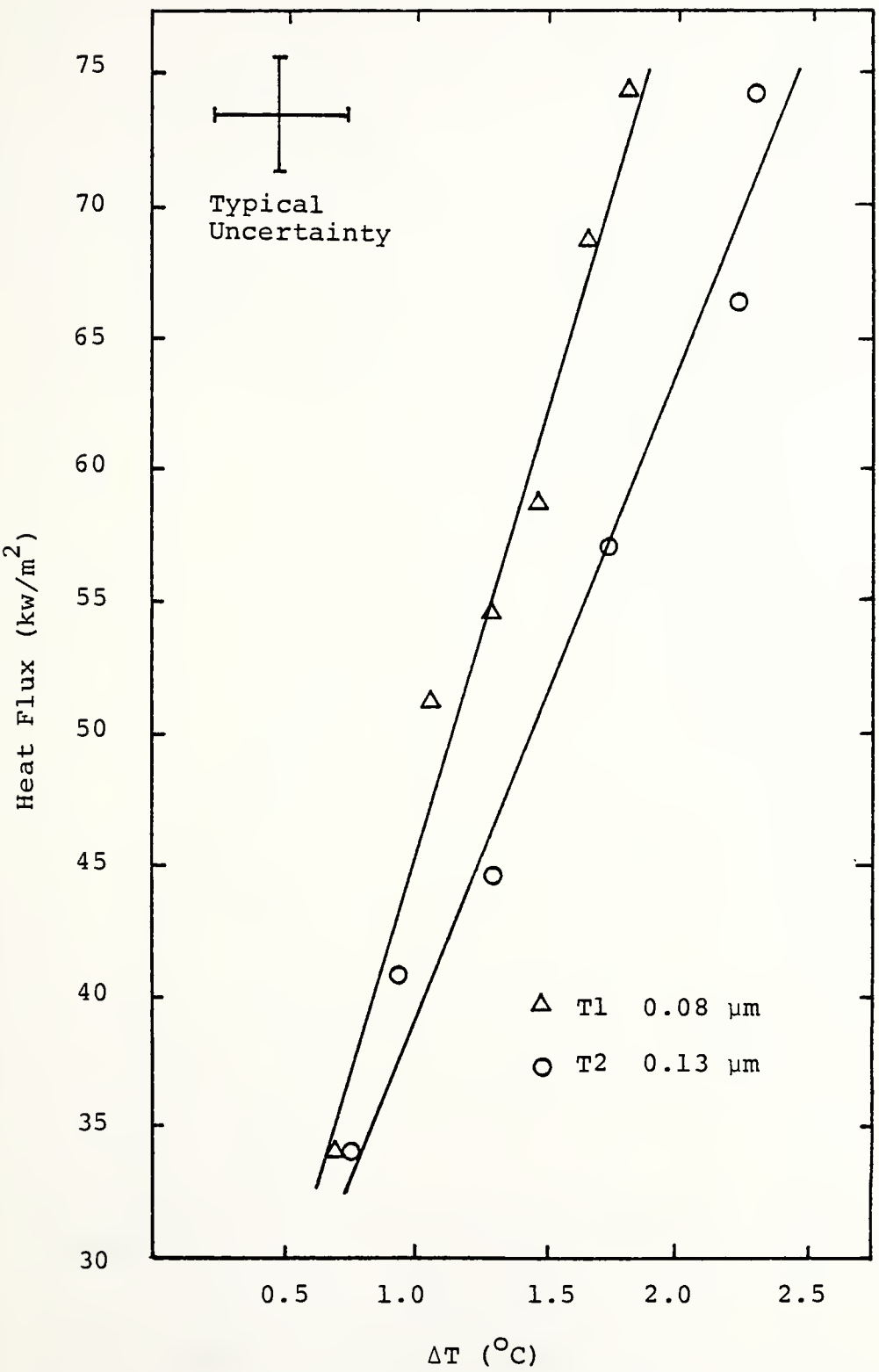

Figure 11. Heat Flux vs. ΔT for the Sputtered Teflon Coatings on Copper-Nickel Specimens.

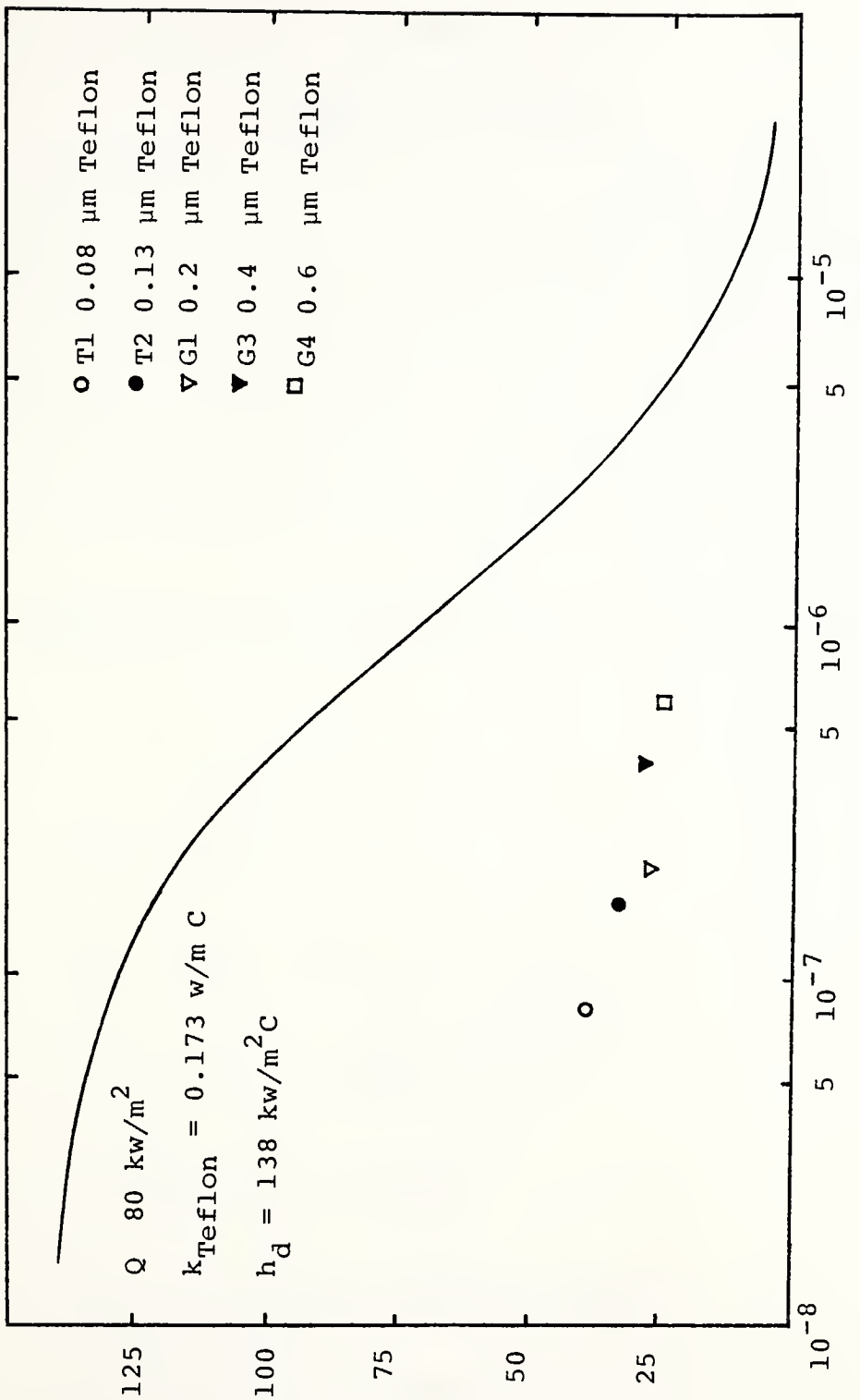

Figure 12. Coating Thickness vs. Heat Transfer Coefficient.

APPENDIX A

UNCERTAINTY ANALYSIS

The uncertainty in heat flux and surface temperature were determined using standard statistical techniques. Miller and Freund [19] were the source for the basic equations. The uncertainty in surface temperature was also calculated using the Wilcox method [20], because it is almost universally used. The uncertainty in the heat transfer coefficient was calculated using the method of Kline and McClintock [21].

A.1. Uncertainty in Surface Temperature and Heat Flux

$$T = T_o + mx$$

$$S_{xx} = n\sum_{i=1}^{n} x^2_i - (\Sigma x_i)^2$$

$$S_e^2 = \frac{1}{n-2} \sum_{i=1}^{n} [T_i - (T_o + mx)]^2$$

$$\sigma_T = \pm t\alpha/_2 \cdot S_e \sqrt{\frac{S_{xx} + (n\bar{x})^2}{n\, S_{xx}}}$$

$$\sigma_m = \pm t\alpha/_2 \cdot S_e \sqrt{\frac{n}{S_{xx}}}$$

$t\alpha/_2 = 1.638$ (0.8 confidence level)

σ_T = The uncertainty in the surface temperature

σ_m = The uncertainty in the slope $\frac{\Delta T}{\Delta x}$

$\sigma_q = \sigma_m \cdot k$

A.2. Uncertainty in Heat Transfer Coefficient

$$\sigma_h = \left[\left(\frac{\Delta\, q/A}{q/A}\right)^2 + \left(\frac{\Delta T}{T}\right)^2\right]^{\frac{1}{2}}$$

σ_h = The uncertainty in heat transfer coefficient

A.3. Wilcox Method

$$T_s - \bar{T}_s = S_w \frac{Q/A}{k} d$$

$$S_w = S\sqrt{\frac{1}{n} + \frac{\mu^2}{\Sigma(x_i - \mu)^2}}$$

$$\mu = \frac{1}{n} \Sigma \bar{x}_i$$

n = Number of thermocouples

d = Thermocouple hole diameter

$\bar{x}_i$ = Distance of the ith hole from the wall

A.4. Range of Uncertainties

Using the Wilcox method [20], the uncertainties in surface temperature are as follows:

Copper $\pm 0.05^{\circ}C$

Cu-Ni $\pm 0.28^{\circ}C$

Ti $\pm 0.30^{\circ}C$

Using the standard statistical techniques, the uncertainties in heat flux and surface temperature varied as follows:

Surface Temperature 0.2 to $0.4^{\circ}C$

Heat Flux 1500 to 3500 w/m^2

APPENDIX B

CALCULATION OF THE EXPECTED HEAT TRANSFER COEFFICIENT

For the chemically promoted specimens, the conduction resistance through the promoter was assumed to be negligible. It was also assumed that the heat transfer coefficient, h_e, was the same as that for the permanent promoters. An overall heat transfer coefficient was calculated by adding the conduction resistance in series with the condensation resistance. This assumes one dimensional heat flux.

$$h_e = \frac{1}{(\frac{\Delta x}{k_t} + \frac{1}{h_d})}$$

h_e = Expected heat transfer coefficient

Δx = Promoter thickness

k_t = Thermal conductivity of Teflon

h_d = Condensation heat transfer coefficient for Cu-Ni

Figure 12 shows this result graphically for Teflon and C-6.

$k_t = 0.00017$ kw/$_m{}^oC$ (Teflon)

$h_d = 138$ kw/$_m{}^2{}^oC$

$$h_e = \frac{1}{(\frac{\Delta x}{0.00017} + \frac{1}{138})}$$

Δx was varied from 10^{-8} to 10^{-5} meters.

h_e kw/m c	Δx (meters)
136.0	10^{-8}
135.8	2×10^{-8}
132.6	5×10^{-8}
127.6	10^{-7}
118.7	2×10^{-7}
98.2	5×10^{-6}
76.2	10^{-6}
52.6	2×10^{-5}
27.3	5×10^{-6}
15.1	10^{-5}
8.0	2×10^{-5}
3.3	5×10^{-5}

APPENDIX C

SAMPLE CALCULATIONS

A. A set of sample calculations is performed to illustrate how data was processed for specimen G3.

1. Physical and Geometric Properties.

$A_s = 7.92 \times 10^{-4}\ m^2$

$k = 56.0\ w/m^{\circ}C$

$h_{fg} = 2.36 \times 10^{6}\ J/kg$

$x_i = 0.00254$ m (spacing between thermocouples)

V_c = volume of Teflon cup = 12.5 cc

2. Raw Data

Thermocouples

No.	Position No.	Reading (mv)	Temp. (°C)
3	T_v	2.395	58.99
13	6	2.207	54.25
14	5	2.220	54.53
15	4	2.106	51.67
16	3	1.998	49.00
17	2	1.897	46.77
18	1	1.772	43.70

Condensate Flow Rate

Run #1 t = 740 sec.

Run #2 t = 675 sec.

The temperature was obtained using the IBM, IMSL Subroutine INTERPL with the thermocouple calibration data. Thermocouples #5 and #6 were at the same axial position, so their average value was used.

Position No.	Thermocouple Temp. (^{o}C)	Distance from Surface (m)
5, 6	54.39	0.00254
4	51.67	0.00508
3	49.00	0.00762
2	46.77	0.01016
1	43.70	0.01270

The above data was evaluated by the method of least squares. A Texas Instrument TI-58 calculator with a built-in linear regression program was used.

$$T_s = 56.99^{o}C$$

$$\frac{\Delta T}{\Delta x} = -1034.65^{o}C/_{m}$$

$$\frac{Q}{A} = -k \frac{\Delta T}{\Delta x} = -(56) \ (-1034.65) = 57.9 \ kw/_{m^2}$$

$$h = \frac{\frac{Q}{A}}{T_v - T_s} = \frac{57.9}{(58.99 - 56.99)}$$

$$h = 29.0 \ kw/_{m^2 o_C}$$

Calculation of heat flux from condensate collection data.

$$Q = \dot{m} \ hfg$$

$$\dot{m} = \frac{m}{t}$$

$$m = \rho V_c$$

$$m = (983.28) \ (12.5 \times 10^{-6}) = 0.123 \ kg$$

Run #1 t = 740 sec.

$$Q = \frac{(0.0123)\ (2.36 \times 10^{+6})}{740} = 39.2\ \frac{J}{S}$$

$$\frac{Q}{A} = \frac{39.2}{7.92 \times 10^{-4}}$$

$$\frac{Q}{A} = 49.5\ kw/_{m^2}$$

Run #2

$$\frac{Q}{A} = 54.3\ kw/_{m^2}$$

$$\therefore \frac{Q}{A}_{avg.} = 51.9\ kw/_{m^2}$$

B. Uncertainty Calculations

1. Wilcox method

$$S_w = S\sqrt{\frac{1}{n} + \frac{\mu^2}{\Sigma(x_i - \mu)^2}}$$

$S = 0.31$

$n = 5$

$\mu = \frac{1}{n} \sum^{n} \bar{x}_i$

$\mu = 0.00762$

$$S_w = 0.31\sqrt{\frac{1}{5} + \frac{5.80 \times 10^{-5}}{6.45 \times 10^{-5}}}$$

$S_w = .325$

$T_s - \bar{T}_s = S_w \frac{Q/A}{k} d$

$$T_s - \bar{T}_s = .325\ \frac{57.940}{56}\ 5.713 \times 10^{-4}$$

$$T_s - \bar{T}_s = 0.19^{o}C$$

2. Standard Statistical Method

$$T = T_o + m_x$$

$$S_{xx} = n\Sigma\, x_i^{\,2} - (\Sigma\, x_i)^2$$

$$S_{xx} = 3.23 \times 10^{-4}$$

$$S_e^{\,2} = \frac{1}{n-2}\,\Sigma\,[T_i - (T_o + m_x)]^2$$

$$\sigma_T = t_{\alpha/2} \cdot S_e \sqrt{\frac{S_{xx} + (n\bar{x})^2}{n\, S_{xx}}}$$

$$\sigma_T = (1.638)\ (0.20) \sqrt{\frac{(3.23 \times 10^{-4}) + [(5)\ (0.00762)]^2}{(5)\ (3.23 \times 10^{-4})}}$$

$$\sigma_T = \pm\ 0.34^{o}C$$

$$\sigma_m = t_{\alpha/2} \cdot S_e \sqrt{\frac{n}{S_{xx}}}$$

$$\sigma_m = (1.638)\ (0.20) \sqrt{\frac{5}{3.23 \times 10^{-4}}}$$

$$\sigma_m = 41.4\ \frac{^{o}C}{m}$$

$$\sigma_{Q/A} = 2{,}319\ \frac{w}{m^2}$$

$$\sigma_h = \left[\left(\frac{\sigma_T}{T}\right)^2 + \left(\frac{\sigma_{Q/A}}{Q/A}\right)^2\right]^{\frac{1}{2}}$$

$$\sigma_h = \left[\left(\frac{0.34}{2}\right)^2 + \left(\frac{2{,}319}{57{,}940}\right)^2\right]^{\frac{1}{2}}$$

$$\sigma_h = \pm 5{,}059\ \frac{w}{m^{2\,o}C}$$

APPENDIX D

NUSSELT ANALYSIS

The basic Nusselt equation for a flat plate was used.

$$\bar{h}_L = 0.943 \left[\frac{\rho_f^2 \, h_{fg} (k_f)^3}{L(x) \, \mu_f \, (T_v - T_s)}\right]^{\frac{1}{4}}$$

$T_V = 60^{\circ}C$

$T_s = 58^{\circ}C$

$\Delta T = 2^{\circ}C$

$h_{fg} = 2.36 \times 10^{-6} \; J/_{kg}$

$k_f = 0.654 \; w/_{m^{\circ}C}$

$\rho_f = 983.2 \; kg/_{m^3}$

$\mu_f = 5.13 \times 10^{-4} \; kg/_{m \cdot s}$

$g = 9.8 \; m/_{s^2}$

$$\bar{h}_L = 8332 \left(\frac{1}{L(x)}\right)^{\frac{1}{4}}$$

Because the surface is circular, $\bar{h}_L$ will vary across the surface. The average value was obtained by integrating $\bar{h}_L$ over the area and dividing by the area.

$$\bar{h}_{disc} = \frac{\int \bar{h}_{L(x)} \, dA}{A}$$

$$\bar{h}_{L(x)} = \frac{8332}{L(x)^{\frac{1}{4}}}$$

$L(x) = 2R\cos\theta$, R = The radius of the disc

$$R = 0.01588m$$

$$dA = L(x)dx$$

$$\bar{h}_{disc} = \frac{1}{2\pi R^2} \int_0^{\pi} \frac{(8332)\ (2R\cos\theta)\ (2R\cos\theta)}{2(2R\cos\theta)^{\frac{1}{4}}}\, d\theta$$

$$\bar{h}_{disc} = 20.80\ kw/_{m^2 o_C}$$

BIBLIOGRAPHY

1. Search, H. T., A Feasibility Study of Heat Transfer Improvement in Marine Steam Condensers, MSME, Naval PostgraduateSchool, Monterey, Ca., December 1977.

2. Jakob, M., "Heat Transfer in Evaporation and Condensation-II," Mechanical Engineering, Vol. 58, 1936, pp729-739.

3. Tamman, G., and Boehme, W.,"Die Zahl der Wassertropfehen bei der Kondensation auf ver schiedenen festen stoffen," Annalen der Physic, Vol. 5, 1935, pp77-80.

4. Graham, C., and Aerni, W. F., "Dropwise Condensation: A Heat Transfer Process for the '70s," Naval Ship Systems Command Tech. News, Vol. 19, July, 1970, pp. 8-15

5. Tanasawa, I., "Dropwise Condensation: The Way to Practical Applications," Sixth International Heat Transfer Conference, Vol. 6, Toronto, Canada, August 1978.

6. Hannemann, R. J. and Mikic, B. B., "An Experimental Investigation of the Surface Thermal Conductivity on the Rate of Heat Transfer in Dropwise Condensation," Int. J. Heat Mass Transfer, Vol 19, 1976, pp 1309-1317.

7. Rose, J. W., "Further Aspects of Dropwise Condensation Theory," Int. J. of Heat Mass Transfer, Vol. 19, No. 12 December 1976.

8. Graham, C., The Limiting Transfer Mechanisms of Dropwise Condensation, Ph.D., MIT, Cambridge , Mass., March 1969.

9. Erb, R. A., and Thelen, E., "Dropwise Condensation," First International Symposium on Water Desalination, Washington, D. C. October 1965.

10. Wilkins, D. G., Bromley, L. A., and Read, S.M., "Dropwise and Filmwise Condensation of Water Vapor on Gold," AIChE Journal, Vol19, No. 1, January 1973, pp. 119-123.

11. Woodruff. D. W., and Westwater, J. W., "Steam Condensation on Electroplated Gold: Effect of Plating Thickness," Int. J. Heat Transfer, Vol. 22., 1979, pp. 627-632.

12. Smith, G. F., Promotion of Dropwise Condentation by Teflon Coated Tubes, U. S. Naval Engineering Experimentation Station, Annapolis, Md., Evaluation Report 030038B, NS-643-078, 12 Oct. 1956.

13. Coxe, E. F., Investigation of the Use of Non-Wetting Agents for Promoting Dropwise Condensation By Teflon Coated Condenser Tubes, Westinghouse Electric Corp., Lester Works, Heat Transfer Department, Engineering Memo EM-377, 19 May 1959.

14. Manvel, J. T., An Experimental Study of Dropwise Condensation on Horizontal Condenser Tubes, MSME, Naval Postgraduate School, Monterey, Ca., June 1979.

15. Sharp, L. R., An Apparatus to Measure Dropwise Condensation Heat Transfer Coefficients of Steam, MSME, Naval Postgraduate School, Monterey, Ca. March 1978.

16. Tanner, D. W., "Heat Transfer in Dropwise Condensation at Low Steam Pressures in the Absence and Presence of Non-Condensable Gas," Int. J. Heat Mass Transfer, Vol. 11, 1967, pp. 181-190.

17. Morgan, J. M., Some Experimental Observations of Dropwise Condensation of Steam, MSME, U. S. Naval Postgraduate School, Monterey, Ca. March 1977.

18. Griffith, J., Naval Research Laboratory Chemistry Division, Washington, D. C., Private Communication.

19. Miller, J., and Freund, J. E., Probability and Statistics for Engineers, 2nd ed., Prentice-Hall, 1977.

20. Wilcox, S. J., and Rohsenhow, W. M., "Film Condensation of Potassium Using Copper Condensing Block for Precise Wall Temperature Measurement," Trans. ASME, Journal of Heat Transfer, Vol. 92, 1970, p. 359.

21. Kline, S. J., and McClintock, F.A.,"Describing Uncertainties in Single Sample Experiments," Mechanical Engineering, Vol. 74 pp. 3-8, Jan. 1953.

22. Heat Transfer Data Book, General Electric Company, Schenectady, NY, 1977, p. 515.23-3.

23. Touloukian, Y. S., Thermophysical Properties of Matter Vol.1, IFI/Plenum, New York, 1970, p. 81, 414.

24. Holman, J. P., Heat Transfer, 4th ed. McGraw-Hill, 1976.

25. Reynolds, W. C., and Perkins, H. C., Engineering Thermodynamics, 2nd ed. McGraw-Hill, 1977.

INITIAL DISTRIBUTION LIST

		No. Copies
1.	Defense Technical Information Center Cameron Station Alexandria, Virginia 22314	2
2.	Library, Code 0142 Naval Postgraduate School Monterey, California 93940	2
3.	Department Chairman, Code 69 Department of Mechanical Engineering Naval Postgraduate School Monterey, California 93940	2
4.	Office of Research Administration, Code 012A Naval Postgraduate School Monterey, California 93940	1
5.	Professor Paul J. Marto, Code 69Mx Department of Mechanical Engineering Naval Postgraduate School Monterey, California	20
6.	LT John T. Manvel, Jr. Supervisor of Shipbuilding, Conversion and Repair Newport News, Virginia 23607	1
7.	Mr. Charles Miller Naval Sea Systems Command (0331) 2221 Jefferson Davis Highway, CP#6 Arlington, Virginia 20360	1
8.	Mr. Walter Aerni Naval Ship Engineering Center (6145) Washington, DC 20360	1
9.	Mr. Wayne L. Adamson Naval Ship Research and Development Center (2761) Annapolis, Maryland 21402	1
10.	Dr. David Eissenberg Oak Ridge National Laboratory Post Office Box Y Oak Ridge, Tennessee 37830	1

11. Miss Eleanor J. Macnair — 1
Ship Department
Ministry of Defence
Director - General Ships, Block B
Foxhill, Bath, Somerset
ENGLAND

12. Professor A. E. Bergles — 1
Department of Mechanical Engineering
Iowa State University
Ames, Iowa 50010

13. Professor James G. Knudsen — 1
Engineering Experimental Station
Oregon State University
Covell Hall-219
Corvallis, Oregon 97331

14. Mr. M. K. Ellingsworth — 1
Office of Naval Research
800 N. Quincy Street
Arlington, Virginia 22217

15. Mr. John Michele — 1
Oak Ridge National Laboratory
Oak Ridge, Tennessee 37830

16. Dr. Win Aung — 1
Division of Engineering, National Science Foundation
1800 "G" Street NW
Washington, DC 20550

17. Dr. James Griffith — 1
Chemistry Division
Naval Research Laboratory
Washington, DC 20550

18. Dr. Theodore Corvino — 1
General Magnaplate Corporation
1331 U.S. Route 1
Linden, New Jersey 07036

19. Dr. Ralph Webb — 1
Department of Mechanical Engineering
Pennsylvania State University
University Park, Pennsylvania 16802

20. Dr. John Rose — 1
University of London
Department of Mechanical Engineering
London E1 4NS
ENGLAND

21. LT Kevin Perkins, USN — 2
U.S. Naval Ship Repair Facility
P.O. Box 8
FPO Seattle, Washington 98762

22. Dr. Garret Vanderplaats, Code 69Vd — 1
Department of Mechanical Engineering
Naval Postgraduate School
Monterey, California 93940

23. Dr. J. W. Westwater — 1
Department of Chemical Engineering
University of Illinois
Urbana, Illinois 61801

Thesis 186503
P3377 Perkins
c.1 An experimental study of dropwise condensation on vertical discs.